Identification of regulatory genes through global gene expression analysis of a *Helicobacter pylori* co-culture system

Nuria Tubau-Juni[1], Josep Bassaganya-Riera[1], Andrew Leber[1], Victoria Zoccoli-Rodriguez[1], Barbara Kronsteiner[1], Monica Viladomiu[1], Vida Abedi[1] and Raquel Hontecillas[1]

[1]Nutritional Immunology and Molecular Medicine Laboratory (www.nimml.org), Biocomplexity Institute of Virginia Tech, Blacksburg, Virginia, United States of America.

Correspondence: Dr. Raquel Hontecillas DVM, PhD, Nutritional Immunology and Molecular Medicine Laboratory (www.nimml.org), Virginia Tech, Blacksburg, VA 24060, USA. E-mail: rmagarzo@vt.edu; phone: (540) 231-7276.

Abstract

Helicobacter pylori is a gram-negative bacterium that establishes life-long infections by inducing immunoregulatory responses. We have developed a novel *ex vivo H. pylori* co-culture system to identify new regulatory genes based on expression kinetics overlapping with that of genes with known regulatory functions. Using this novel experimental platform, in combination with global transcriptomic analysis, we have identified five lead candidates, validated them using mouse models of *H. pylori* infection and *in vitro* co-cultures under pro-inflammatory conditions. Plexin domain containing 2 (*Plxdc2*) was selected as the top lead immunoregulatory target. Gene silencing and ligand-induced activation studies confirmed its predicted regulatory function. Our integrated bioinformatics analyses and experimental validation platform has enabled the discovery of new immunoregulatory genes. This pipeline can be used for the identification of genes with therapeutic applications for treating infectious, inflammatory, and autoimmune diseases.

Introduction

Chronic bacterial infections trigger complex and dynamic host-bacterial interactions that modulate immunometabolic host responses. The phenotypic manifestation of these dynamic interactions results from the coordinated expression of blocks of genes with overlapping functions that cooperate in modulating host responses. In addition to pathogen-associated molecular patterns (PAMPs) that signal infection and are associated with induction of innate anti-bacterial and inflammatory responses, other lesser known bacterial components elicit compensatory immunoregulatory responses that when exploited by pathogens, promote bacterial persistence. For instance, *Mycobacterium tuberculosis* induces IL-10-driven regulatory responses that suppress the activated immune mechanisms and contribute to long-term infection (Gong et al., 1996; Moreira-Teixeira et al., 2017; O'Leary, O'Sullivan, & Keane, 2011; Redford, Murray, & O'Garra, 2011). Therefore, the activation of host

44 immunoregulatory mechanisms by certain bacterial organisms inhibit the effector immune response
45 and prevent bacterial clearance.
46
47 *Helicobacter pylori* is a gram-negative, microaerophilic, spiral-shaped bacterium with unipolar,
48 sheathed flagella (Kusters, van Vliet, & Kuipers, 2006; O'Rourke & Bode, 2001) that constitutes the
49 primary member of the gastric mucosa in infected individuals (Noto & Peek, 2017; Sheh & Fox, 2013).
50 *H. pylori* is highly specialized to colonize the human gastric niche. The infection is chronic and affects
51 more than 50% of the world's population (Hooi et al., 2017). *H. pylori* infection is mostly asymptomatic;
52 however, approximately 10% of carriers will develop peptic ulcers (Ernst & Gold, 2000; Wroblewski,
53 Peek, & Wilson, 2010), and 1-3% gastric cancer (Wroblewski et al., 2010). Interestingly, *H. pylori*
54 infection may be an important driver of systemic tolerance in asymptomatic individuals with an inverse
55 correlation between the presence of this bacterium and the development of autoimmune diseases,
56 asthma, esophageal adenocarcinoma and type-2-diabetes (Bassaganya-Riera et al., 2012; de Martel
57 et al., 2005; Reibman et al., 2008; van Wijck et al., 2018; Xie et al., 2013). These conflicting
58 implications may stem from the relative predominance of antagonistic immune responses that
59 encompass both effector and regulatory components elicited by *H. pylori (Bhuiyan et al., 2014;*
60 *Kabisch, Semper, Wustner, Gerhard, & Mejias-Luque, 2016; Raghavan & Quiding-Jarbrink, 2012;*
61 *Smythies et al., 2000).* However, long-term colonization by the bacterium, due to the failure of the
62 immune system to clear the infection, suggests that the strong *H. pylori*-induced regulatory responses
63 can shift inflammatory/effector responses leading to chronicity of the infection.
64
65 Macrophages have been described as key immune cells in *H. pylori*-induced regulatory mechanisms
66 (Leber et al., 2016). Particularly, *H. pylori* interacts with a specific subset of mononuclear phagocytes
67 that generate IL-10-driven regulatory responses facilitating optimal colonization of the gastric mucosa
68 (Viladomiu et al., 2017). We demonstrated that macrophage peroxisome proliferator-activated
69 receptor gamma (PPARγ), an anti-inflammatory transcription factor, was needed for the induction of
70 the full spectrum regulatory response (Viladomiu et al., 2017). Additional macrophage-expressed

71 genes (*Par1*, *HO-1*) have been shown to play a similar role to PPARγ and contribute to keeping high
72 levels of colonization while reducing pathology and disease (Chionh et al., 2015; Gobert et al., 2014).
73
74 Early after the initiation of the immune response, both macrophages and dendritic cells (DC) endure
75 strong metabolic and transcriptional changes. To increase the speed of energy production and
76 facilitate the execution of effector responses, activated macrophages are subjected to a metabolic
77 switch, in which glycolysis and lactate production predominate, while Krebs cycle and oxidative
78 phosphorylation are reduced into secondary roles (Kelly & O'Neill, 2015; Rodriguez-Prados et al.,
79 2010). This substantial change implies that the metabolic shift towards higher glucose consumption
80 and glycolysis rate is key to enable the required spectrum of host responses in inflammatory
81 macrophages. In contrast, alternatively-activated macrophages present a metabolic component in
82 which oxidative phosphorylation is dominant and fatty acid consumption is increased (Jha et al., 2015;
83 Kelly & O'Neill, 2015; Vats et al., 2006). Moreover, IL-10 was found to suppress glycolysis while
84 stimulating oxidative metabolism (Ip, Hoshi, Shouval, Snapper, & Medzhitov, 2017), suggesting that
85 some metabolic changes are essential for the induction of regulatory responses in macrophages.
86 Interestingly, PPARγ-driven regulatory responses encompass a profound metabolic component since
87 PPARγ is required for glucose and fatty acid uptake, achieve greater fatty acid β-oxidation in
88 macrophages and maintain mitochondrial biogenesis, both dominant processes in alternatively
89 activated macrophages (Odegaard et al., 2007). These metabolic changes are tightly coupled to the
90 suppression of proinflammatory gene expression (Namgaladze et al., 2014; Vats et al., 2006).
91
92 Transcriptional changes play crucial roles in modulating immunomodulatory and metabolic responses
93 to infection. Gene expression is highly coordinated in time, with sets of genes with overlapping roles
94 sharing the same expression pattern by being upregulated and downregulated simultaneously. The
95 loss of a single gene can affect the equilibrium of the whole system and have a significant impact in
96 the outcome of the response. Indeed, suppression or inactivation of a single regulatory protein, for
97 instance PPARγ, results in stronger inflammation, while activation or enhanced expression leads to a

98 balanced response, maintained by induction of immunoregulation (Hontecillas et al., 2011; Odegaard
99 et al., 2007; Viladomiu et al., 2017; Viladomiu et al., 2012).
100
101 In this study, we used an *ex vivo H. pylori* co-culture system to identify genes with putative regulatory
102 function based on the kinetic pattern of expression of known genes using WT and PPARγ-deficient
103 bone marrow-derived macrophages (BMDM). Using a global transcriptomic assay together with a
104 bioinformatics pipeline based on expression pattern-analysis approaches, we have identified five
105 potential new regulatory genes. Extensive *in vitro* and *in vivo* validation studies, in both pro-
106 inflammatory as well as regulatory-induced conditions, support the regulatory functions of the selected
107 group of candidate genes. In particular, the plexin domain containing 2 (Plxdc2) gene was selected
108 as the lead immunoregulatory target, based on its characteristics and expression pattern, for further
109 validation of its regulatory behavior. In conclusion, this manuscript establishes a novel integrated
110 platform for the identification of genes such as *Plxdc2* with promising regulatory and immunometabolic
111 functions that could become new molecular targets to treat inflammatory and autoimmune diseases.
112
113 ## Results
114
115 ### *H. pylori* induces expression of regulatory genes in WT but not in PPARγ-deficient
116 ### macrophages.
117 The *in vivo* interplay between *H. pylori* and the myeloid cell compartment revealed that macrophages
118 are highly responsive to *H. pylori*-induced regulatory responses (Viladomiu et al., 2017). Here, we
119 sought to explore *H. pylori* interactions with macrophages employing a synchronized gentamycin
120 protection co-culture system comparing cells obtained from WT and PPARγ fl/fl;LysCre+ (LysCre+)
121 mice. Gentamycin was applied to the culture system 15 min after cells were exposed to live *H. pylori*
122 to avoid constant extracellular stimulation and synchronize the cellular response. Of note, *H. pylori*
123 can be internalized and replicate in the intracellular compartment (Chu, Wang, Wu, & Lei, 2010; Oh,
124 Karam, & Gordon, 2005; Tang et al., 2012; Wang, Wu, & Lei, 2009). Here, we used intracellular

125 replication post-gentamycin treatment as a marker of the effect and status of the anti-bacterial
126 response. LysCre+ mice lack PPARγ transcription factor in myeloid cells, which results in defective
127 expression of genes with regulatory function and overexpression of pro-inflammatory and anti-
128 bacterial response genes (Guirado et al., 2018; Malur et al., 2009; Szanto et al., 2010). Cells were
129 harvested at several time-points from 0 to 12 hours post-gentamycin exposure to assess the bacterial
130 burden and changes in gene expression in response to *H. pylori*. The same pattern of bacterial
131 replication was observed for both genotypes. Initial replication was first detected 30 min post-
132 gentamycin treatment and the peak occurred at 120 min (**Figure 1A**). However, bacterial counts in
133 co-cultures of LysCre+ macrophages were significantly reduced throughout the time course, starting
134 at 60 min post-challenge and up to 240 min post-challenge. This phenotype was compatible with an
135 inflammatory shift in LysCre+ BMDM due to the loss of PPARγ resulting from altered activation of
136 certain regulatory *H. pylori*-induced mechanisms and consequently a more efficient anti-bacterial
137 response. To validate this assessment, WT and LysCre+ macrophages were classically activated
138 through LPS/IFNγ stimulation 24 hours prior to the infection. Generation of pro-inflammatory WT
139 macrophages resulted in drastic suppression of *H. pylori* loads at the 120 min time point, compared
140 to the WT control (**Figure 1B**). Moreover, the bacterial burden peak was entirely abrogated in
141 LPS/IFNγ-treated LysCre+ cells. Regarding the *H. pylori*-induced gene expression profile, IFNγ
142 expression following *H. pylori* challenge was remarkably increased in LysCre+ cells compared to WT.
143 The WT group showed a minimal increase at all timepoints relative to time 0 (**Figure 1F**). In contrast,
144 WT macrophages displayed a dramatic increase of the anti-inflammatory cytokine IL-10 at 60 min
145 post-*H. pylori* co-culture, that was significantly diminished in LysCre+ BMDM (**Figure 1E**). Therefore,
146 *H. pylori* promotes the activation of cytokine-driven regulatory mechanisms in WT macrophages, that
147 modulate the immune response and generate a regulatory microenvironment that facilitates bacterial
148 proliferation reaching the highest peak at 2 hours post gentamycin treatment.
149
150 To elucidate the underlying regulatory molecular mechanisms activated upon *H. pylori* co-culture in
151 WT macrophages, we performed a global transcriptomic analysis on a gentamycin protection assay

time course (0, 60, 120, 240, 360 and 720 min). RNAseq analysis demonstrated important differences in the gene expression profile within both genotype (**Figure 1C**) and treatment (**Figure 1D**). Almost 50% of genes exhibited a significant differential expression based on the treatment, with a substantial upregulation after *H. pylori* challenge. Thus, *H. pylori* strongly influences the macrophage transcription profile, resulting in drastic modifications in macrophage function that favor the generation of a regulatory phenotype. Therefore, we sought to utilize the new co-culture system to explore novel regulatory pathways activated upon *H. pylori* infection to discover new host regulatory genes that modulate the immune response, with the potential to become molecular targets for the development of therapeutics for infectious, inflammatory and autoimmune diseases.

Validation of experimental co-culture system with identification of differential expression patterns in characterized antimicrobial genes.

Expression of regulatory and pro-inflammatory genes is tightly regulated and coordinated over time. Indeed, these sets of genes frequently present opposite expression kinetics under the same conditions. We selected nine established canonical pro-inflammatory genes to initially explore and identify distinctive patterns of expression associated with pro-inflammatory and antimicrobial functions. Inflammation-related genes are characterized by an increased expression level in *H. pylori*-infected groups compared to the controls (**Figure 2 – figure supplement 1**), and in the majority of genes, *H. pylori*-induced upregulation is achieved at the later time points of the co-culture (**Figure 2 – figure supplement 1B-F, H-I**). As expected, lack of PPARγ results in higher gene expression of pro-inflammatory genes. We then performed a 3-way ANOVA analysis that reported the differential expression of eight genes, including *Chil1*, *Etv5*, *Iigp1*, *Ptger4*, *Sqle*, *Osm*, *Rptoros* and *Hspa2* (**Figure 2 – figure supplement 2**). Most of the genes revealed by the 3-way ANOVA are associated with known pro-inflammatory functions. We focused our analysis in *Chil1* (**Figure 2 – figure supplement 2A**), *Iigp1* (**Figure 2 – figure supplement 2C**) and *Sqle* (**Figure 2 – figure supplement 2E**) due to their expression kinetics that resemble the identified inflammatory genes pattern and their well-known associated role to the host response against pathogens. RNAseq validation through qRT-PCR revealed a similar expression pattern in *Chil1* and *Iigp1*, characterized by a later upregulation

due to the infection in both genotypes in case of *ligp1* (**Figure 2E**) or only in infected LysCre+ cells in case of *Chil1* (**Figure 2D**). In contrast, the later induction of *Sqle* following *H. pylori* challenge, was undetectable in the qRT-PCR analysis (**Figure 2F**), which resulted in no differences within groups among the entire time course. In addition, *Chil1* and *ligp1* gene silencing (**Figure 2 – supplement 3A-B**) led to a definite increase of bacterial loads in both genotypes (**Figure 2G**). Indeed, the significant decrease of bacterial burden in LysCre+ macrophages, when compared to the WT group, was abrogated due to *Chil1* or *ligp1* gene knockdown. As expected, there were no differences in culture systems due to silencing of *Sqle*. Therefore, the initial analysis of this global transcriptomics dataset based on patterns of expression related to pro-inflammatory functions highlighted two genes, *Chil1* and *ligp1*, with a relevant, previously established role in macrophage antimicrobial responses. Thus, it validated the potential use of this co-culture system for the identification of novel host immunoregulatory genes by means of kinetic pattern analysis within genotypes and among the time course.

Bioinformatics pattern-expression analysis identified five candidates as novel genes with putative regulatory functions.

Nod-like receptors (NLRs) are a subfamily of pattern recognition receptors that like PPARs, regulate innate immune responses and metabolism. Upon ligand binding, downstream activation of the NLR pathway results in the initiation and regulation of potent inflammatory mechanisms, including inflammasome formation and NF-κB activity (Kim, Shin, & Nahm, 2016; Zhong, Kinio, & Saleh, 2013). NLR and PPAR canonical immune pathways were selected to identify the opening set of expression patterns of interests. NLR and PPAR pathways encompass more than 200 genes and modulate the immune response through the activation of transcription and/or induction of metabolic changes in immune cells. Further, even the established role of the NLR pathway in innate immunity activation and the PPAR pathway association to regulatory mechanisms, both canonical pathways in-conjunction contain a mixture of genes presenting a dominant pro-inflammatory or anti-inflammatory role, leading to combined expression patterns in the dataset that allows the identification of regulatory patterns.

Initially, we performed an analysis based on the fold change of gene expression between genotypes for each gene of both NLR and PPAR pathways across the entire time course presented in the form of heat maps (**Figure 3A, D**) where blue represents genes downregulated in WT compared to LysCre+, while red represents upregulation of gene expression in WT related to LysCre+. We anticipated the presence of inverted patterns of regulatory and pro-inflammatory genes between both genotypes, where regulatory genes would be increased in WT compared to PPARγ-deficient, and pro-inflammatory genes overexpressed in PPARγ-deficient group. Indeed, the bioinformatics analysis revealed specific expression patterns in both signaling pathways that were clustered in groups. The NLR pathway includes two well-defined clusters based on the distinct genotype gene expression (**Figure 3A**). The orange box, at the top, contains genes upregulated in LysCre+ macrophages, and the green box, at the bottom, contains a second class of genes with greater expression in the WT group. Interestingly, the LysCre+ upregulated genes have a delayed expression pattern, while, WT upregulated genes presented an earlier peak. The two NLR clusters are represented in the PPAR pathway, also depicted in orange and green boxes (**Figure 3D**). The analysis of genes associated with PPAR revealed an additional third cluster, highlighted in purple, including a group of genes characterized by a dysregulated pattern. Particularly, those genes exhibited oscillating expression kinetics in each genotype among the entire time course. A plausible explanation is the existence of a strong PPARγ interaction with these genes. Therefore, the absence of the transcription factor in LysCre+ macrophages could alter the expression of the genes, due to direct activation, inhibition or even due to the upregulation of compensatory mechanisms, that result into a fluctuating expression pattern.

Gene selection was narrowed to the green box cluster (i.e. genes upregulated in WT), to include genes with a positive response to *H. pylori* in WT macrophages that resembled the peak of bacterial loads reported in this genotype (**Figure 1A**). The choice included 7 NLR (**Figure 3B**) and 10 PPAR (**Figure 3E**) pathway genes highlighted in red, which were defined as seed genes. Based on the

235 expression patterns of the seed genes, we built an initial dataset that comprised both these original
236 genes and a group described as linked genes obtained from the global transcriptome dataset. Linked
237 genes are characterized by their similar expression pattern and linked functions to the seed genes.
238 Certain differentially expressed patterns were selected in this large initial dataset, and through 2
239 cycles of clustering within the entire global transcriptional dataset, we obtained a specific group of
240 candidates exhibiting the defined expression kinetics. To further narrow down our search, we utilized
241 the Pubmatrix (Becker et al., 2003) tool to select the most novel genes based on the following criteria:
242 number of publications, cell location, and known function (**Figure 3C**). The 21 genes included in the
243 final set were divided in 5 groups based on their expression pattern (**Figure 3 – figure supplement**
244 **1**). Groups 1 and 2 exhibit a clear distinctive pattern within genotype, whereas no genotype
245 differences were observed in groups 3, 4 and 5 (**Figure 3F**). Further, the first two groups exhibit a
246 drastic upregulation post-*H. pylori* challenge in WT that was abrogated in PPARγ-deficient
247 macrophages. Therefore, genes included in groups 1 and 2 displayed an expression pattern
248 potentially associated with a regulatory function.
249
250 Based on the pattern analysis, five genes from groups 1 and 2 of the final dataset were identified as
251 potential new regulatory leads for further validation. Plexin domain containing 2 (*Plxdc2*, **Figure 4A**),
252 V-set and immunoglobulin domain containing 8 (*Vsig8*, **Figure 4C**), Ankyrin repeat domain 29
253 (*Ankrd29*, **Figure 4D**) and C1q and tumor necrosis factor related protein 1 (*C1qtnf1*, **Figure 4E**) share
254 an early expression peak in WT macrophages, abrogated in LysCre+, that coincides with the bacterial
255 burden spike in the gentamycin protection assay. The kinetics of Protein phosphatase 1 regulatory
256 subunit 3E (*Ppp1r3e*, **Figure 4B**) is slightly different since it was still upregulated in the last timepoint.
257 However, in LysCre+ macrophages, the expression pattern of all five candidates was consistently
258 downregulated and displayed as a flat line. Known properties of these five genes are described in
259 **Table 1**. Publications linked to each of the genes reveal a large diversity of established functions;
260 however, association with the immune system or the immune response was not reported for the
261 majority of the genes. Interestingly, cellular location is also highly heterogeneous. Only two
262 candidates, *Plxdc2* and *Vsig8*, both plasma membrane receptors, have identified ligands. Thus, the

limited number of publications together with the current established function of each gene support the novelty of their potential interaction with host immunoregulatory mechanisms.

In vivo and _in vitro H. pylori_-induced upregulation of all five lead target candidates in WT mice is abrogated in pro-inflammatory macrophages from PPARγ null mice.

To perform a validation of the five selected genes, we initially measured their expression, by qRT-PCR on samples from each time point of the gentamycin protection assay used in the global transcriptomic analysis. Similar to the observed pattern in the RNAseq dataset, *H. pylori* co-culture induces a significant early upregulation of all five candidates in WT macrophages starting at 60 minutes post co-culture. After 60 minutes, the expression of *Plxdc2* (**Figure 5A**), *Vsig8* (**Figure 5E**), *Ankrd29* (**Figure 5G**) and *C1qtnf1* (**Figure 5I**) begin to decline in cells obtained from WT mice to reach same levels as the LysCre+ BMDM at 360 or 720 minutes. Similar to the results from the RNAseq data, *Ppp1r3e* (**Figure 5C**) expression was maintained at high levels throughout the time course analysis. Cultures from LysCre+ BMDM exposed to *H. pylori* failed to upregulate expression of the selected genes. Therefore, there is an early upregulation of the five genes in WT BMDM that was suppressed in cells with a pro-inflammatory phenotype due to the loss of PPARγ.

To explore the dynamics of the selected genes *in vivo*, WT and LysCre+ mice were infected with *H. pylori.* In a previous study, we demonstrated that *H. pylori* infection *in vivo* induces strong regulatory mechanisms driven by IL-10-expressing myeloid cells starting at day 14 post-infection and reaching maximum levels at day 28 post-infection (Viladomiu et al., 2017). To evaluate whether induction of regulatory responses *in vivo* alters the kinetics of targeted genes, stomachs were collected at day 28 from infected and non-infected mice. Consistent with the *in vitro* findings, *H. pylori* infection upregulated the expression of *Plxdc2* (**Figure 5B**), *Ppp1r3e* (**Figure 5D**), *Vsig8* (**Figure 5F**), *Ankrd29* (**Figure 5H**) and *C1qtnf1* (**Figure 5J**) in WT gastric tissue. In contrast, minimal or no differences were reported upon *H. pylori* infection in PPARγ-deficient mice. Therefore, activation of regulatory responses after *H. pylori* challenge in WT mice correlate with increased transcription of the five

selected genes. However, *H. pylori* infection under pro-inflammatory conditions, due to the lack of PPARγ, abrogates this effect on the selected lead regulatory genes.

Activation of pro-inflammatory responses modulate the dynamics of the top lead regulatory target genes.

To further characterize the potential regulatory functions of the selected genes, we sought to assess their behavior under inflammatory conditions in a controlled environment *in vitro*. Briefly, WT and LysCre+ BMDM were treated with 100ng/mL of LPS for 60, 120, 240, 360 and 720 minutes. LPS administration *in vitro* activates BMDM and modulates their cytokine profile. Particularly, LPS upregulates TNFα expression with a significant increment in LysCre+ macrophages (**Figure 6F**). In contrast, the IL-10-induced peak reported in WT macrophages is abrogated by the lack of PPARγ (**Figure 6H**). Additionally, LPS treatment suppressed PPARγ expression starting at 60 minutes post challenge (**Figure 6G**). The results show a slight decrease in *Plxdc2* (**Figure 6A**), *Vsig8* (**Figure 6C**) and *C1qtnf1* (**Figure 6E**) expression after LPS treatment plus a significant downregulation of *Ppp1r3e* starting at 120-minutes post stimulation (**Figure 6B**) in WT compared to PPARγ-deficient macrophages. However, no differences were reported for *Ankrd29* (**Figure 6D**). As opposed to the dramatic modulation of the kinetics reported under a regulatory microenvironment *in vitro,* the effect observed upon LPS stimulation was limited and gene-specific.

***Plxdc2* silencing prevents *H. pylori*-induced regulatory phenotype in macrophages and reduces bacterial burden.**

Once initial screening and validation of the five lead candidates was completed, *Plxdc2* was chosen to further explore its regulatory activity. *Plxdc2* was selected based on the reported expression kinetics under regulatory and pro-inflammatory conditions, together with the fact that *Plxdc2* is a plasma receptor with a known ligand. WT and LysCre+ BMDM were transfected with 20 nM of *Plxdc2* targeted or scrambled siRNA as a negative control using Lipofectamine reagent. BMDM were subjected to the gentamycin protection assay. Cells were harvested at 0, 60, 120, 240 and 360

317 minutes post-challenge for gene expression analysis, and at 120 minutes for assessment of bacterial
318 loads. Gene silencing resulted in 70% efficiency in WT macrophages, reducing *Plxdc2* expression in
319 this group down to the levels observed in PPARγ-deficient BMDM (**Figure 7A**). At 2 hours post co-
320 culture, *Plxdc2* silencing resulted in a 3-fold reduction of *H. pylori* burden in WT macrophages (**Figure**
321 **7D**). Additionally, a lower number of *H. pylori* colonies was isolated from both PPARγ-deficient groups
322 in comparison to the WT. However, within LysCre+ macrophages, no differences in bacterial burden
323 were observed after *Plxdc2* suppression via gene silencing. To assess whether the reduced bacterial
324 replication reported in *Plxdc2*-silenced WT macrophages was due to a potential *Plxdc2* modulation of
325 the macrophage function, we assessed the expression of Arginase 1 (Arg1) and Resistin like alpha
326 (Retnla or fizz1) genes, associated with tissue repair and anti-inflammatory functions in these cells.
327 Both, *Arg1* (**Figure 7B**) and *Retnla* (**Figure 7C**) reported an early response to *H. pylori,* synchronized
328 with the *Plxdc2* expression peak at 60 minutes post-infection in WT Plxdc2-expressing macrophages.
329 However, *Plxdc2* silencing prevented the upregulation of *Arg1* and *Retnla1* after *H. pylori* challenge,
330 leading to a complete abrogation of the 60-minute peak. Similar to the results from bacterial loads, no
331 differences were detected in PPARγ-deficient BMDM irrespective of the state of *Plxdc2* silencing.
332 Indeed, in both LysCre+ groups *Arg1* and *Retnla* exhibited a constant flat expression, also previously
333 observed in all 5 selected candidates (**Figure 5**). Therefore, *Plxdc2* silencing abrogated *H. pylori*-
334 induced regulatory responses in macrophages, resulting in limited bacterial persistence and
335 replication in WT BMDM.
336
337 To further validate the ability of *Plxdc2* to modulate the macrophage phenotype towards a regulatory
338 environment, the *Plxdc2* molecular pathway was activated through the administration of pigment
339 epithelium-derived factor (PEDF), a known Plxdc2 ligand. Interestingly, PEDF treatment slightly
340 increased *Arg1* (**Figure 7E**) and *Retnla* (**Figure 7F**) gene expression in WT and LysCre+
341 macrophages compared to their respective untreated controls. Indeed, the significant downregulation
342 due to the loss of PPARγ in the untreated group was abrogated after PEDF treatment, exhibiting no
343 differences in comparison to the WT control. Additionally, *Arg1* and *Retnla* expression levels were

inhibited in all 4 groups transfected with *Plxdc2* siRNA, reporting no PEDF effects. Therefore, PLXDC2 activation through PEDF treatment increased the expression of anti-inflammatory genes in macrophages and rescued the inflammatory phenotype observed in PPARγ-deficient cells.

Discussion

We present a novel *ex vivo* co-culture system that leverages the regulatory responses induced by *H. pylori* in macrophages in combination with bioinformatics analyses to discover potential new regulatory genes with immunomodulatory properties based on expression kinetics in WT and PPARγ-deficient BMDM. This new platform was used to identify five genes, *Plxdc2*, *Ppp1r3e*, *Vsig8*, *Ankrd29* and *C1qtnf1* with potential regulatory functions. Induction of regulatory responses through *H. pylori* challenge *in vivo* and *in vitro* confirmed the promising regulatory role of the selected genes. Indeed, the hypothesized regulatory pattern utilized to identify the novel genes, characterized by an early upregulation in WT macrophages and suppression in PPARγ-deficient macrophages, coinciding with the early peak of bacterial burden, was observed in all 5 top lead candidates through *H. pylori* validation *in vitro.* Further, *H. pylori* infection *in vivo* resulted in increased gene expression of all 5 top candidates at day 28 post-infection in WT mice, coinciding with the previously identified greatest accumulation of regulatory macrophages in the gastric mucosa during this bacterial infection (Viladomiu et al., 2017). Therefore, functionally, the correlation between the expression of the 5 candidates and the induction of regulatory mechanisms during *H. pylori* infection, support the immunomodulatory role of the selected genes. Moreover, the validation of the co-culture system provides new insights into the application of bioinformatics screening methods for the discovery of novel molecular targets for treating inflammatory and autoimmune diseases.

H. pylori establishes life-long, chronic infections in the gastric mucosa characterized by the induction of mixed immune responses. In addition to the effector mechanisms dominated by Th1 and Th17 cells (Bhuiyan et al., 2014; Carbo et al., 2013; Caruso et al., 2008; D'Elios et al., 1997; Shi et al., 2010;

371 Smythies et al., 2000), *H. pylori* induces strong regulatory responses that suppress mucosal
372 inflammation, contribute to tissue integrity maintenance and prevent effective bacterial clearance
373 (Lundgren, Suri-Payer, Enarsson, Svennerholm, & Lundin, 2003; Raghavan, Fredriksson,
374 Svennerholm, Holmgren, & Suri-Payer, 2003; Raghavan & Quiding-Jarbrink, 2012). Historically, *H.*
375 *pylori*-associated regulatory responses have been mainly attributed to dendritic cells by inhibition of
376 effector T cells and promotion of regulatory T cells (Kabisch et al., 2016; Kaebisch, Mejias-Luque,
377 Prinz, & Gerhard, 2014; Tanaka et al., 2010). Recently, macrophages have been identified as an
378 integral component in the generation of a regulatory gastric microenvironment during this bacterial
379 infection (Leber et al., 2016; Viladomiu et al., 2017). Applying next-generation sequencing (NGS) and
380 bioinformatics analysis, we demonstrated that in the tightly controlled environment of an *ex vivo* co-
381 culture with BMDM, *H. pylori* challenge drastically influence macrophage gene expression profiles.
382 The significant impact observed in macrophage transcriptomics upon bacterial challenge resulted in
383 the induction of regulatory genes in WT macrophages, that is inhibited by the loss of PPARγ and
384 suppresses the effector mechanisms to promote bacterial persistence. Therefore, the synchronized
385 *ex vivo* co-culture with macrophages, together with the utilization of NGS strategies, is a suitable
386 approach to capture the full spectrum of regulatory responses induced by *H. pylori* and to discover
387 novel regulatory mechanisms with a meaningful impact on the modulation of the immune response.
388
389 In addition to the combined NGS and bioinformatics analyses methods, in the current study, gene
390 selection is based on the similarities between the expression kinetics of candidate genes and known
391 host genes with validated regulatory functions. We performed a bioinformatics pattern-based analysis
392 utilizing genes with established regulatory functions to identify novel genes with similar
393 characteristics. In our system, the comparison within macrophages with distinctive immunological
394 steady states (WT versus PPARγ-deficient) was utilized to select the initial core of established genes
395 and to validate the role of the new regulatory gene candidates. To identify the predicted regulatory
396 patterns, we utilized the canonical immune pathways NLR and PPAR. The selection criteria were
397 based on pathways with a dominant regulatory role or including both inflammatory and regulatory

members, to allow the full spectrum of expression kinetics and perform a suitable selection of expression patterns associated with immunomodulatory functions. PPARs are nuclear receptors that regulate lipid metabolism and exert potent immunomodulatory functions. Indeed, activation of members in the PPAR pathway result in incremented beta-oxidation of lipid metabolism and suppression of the inflammatory response (Varga, Czimmerer, & Nagy, 2011). The NLR family is a main regulator of the initiation of innate immune responses in macrophages and encompasses more than 20 members (Zhong et al., 2013). As expected, NLR pathway includes an important number of inflammation-driven genes involved in the formation of inflammasomes, such as NLRP1, NLRP3 and NLRC4 (He, Hara, & Nunez, 2016; Masters et al., 2012) or associated with the activation of other inflammatory mechanisms, mainly the NF-κB or MAPK pathways, such as NOD1 and NOD2 (Zhong et al., 2013). Additionally, several genes of the NLR family hold immunoregulatory functions linked to suppression of inflammation, including NLRP10 and NLRX1 (Imamura et al., 2010; Leber et al., 2018; Leber et al., 2017; Xia et al., 2011). Therefore, NLRs constitute a highly heterogeneous and diverse family of pattern recognition receptors (PPR). Other pathways essential for the activation and maintenance of the immune response in macrophages were also considered, including the Toll-like receptors (TLR), the nuclear factor kB (NF-kB) and pathways associated to the production of reactive oxygen species (ROS). However, the strong association of such pathways with the initiation and expansion of inflammatory mechanisms with limited pro-regulatory functions in macrophages (Kawai & Akira, 2006; Liu, Zhang, Joo, & Sun, 2017), limited their potential value in our regulatory gene discovery pipeline. Therefore, to perform an initial screening analysis for regulatory genes, NLR and PPAR pathways were ideal candidates.

The hypothesized immunomodulatory role of the selected regulatory gene candidates was further investigated under the induction of inflammatory mechanisms. LPS stimulation *in vitro* resulted in minor alteration of the expression kinetics in both genotypes. While we observe a trend in *Plxdc2* and *Ppp1r3e* gene expression that supports the hypothesized suppression of immunoregulatory gene levels in pro-inflammatory activated macrophages, PPARγ-deficient cells exhibited slightly greater expression of *Vsig8, Ankrd29* and *C1qtnf1*. LPS stimulation induces strong pro-inflammatory cytokine

426 production, including TNF, IL-6, and IL1β, and the generation of classically-activated macrophages
427 (Arango Duque & Descoteaux, 2014). Therefore, the minor LPS effect on the selected candidates
428 suggests that they might not be associated with the induction or maintenance of pro-inflammatory
429 responses. In conclusion, the observed results in both *in vivo* and *in vitro* experiments under the
430 induction of regulatory and pro-inflammatory mechanisms, suggest that *Plxdc2* and *Ppp1r3e* are the
431 two genes with greater immunomodulatory potential and the most suitable candidates for further
432 validation and study.
433
434 *Plxdc2* encodes a 350-amino acid plasma membrane protein known to participate in cell proliferation
435 and differentiation control during the development of the nervous system (Miller et al., 2007; Miller-
436 Delaney, Lieberam, Murphy, & Mitchell, 2011). Our results suggest that *Plxdc2* silencing alters the
437 phenotype of WT macrophages *in vitro* causing a shift towards a more pro-inflammatory state, leading
438 to a significant decrease of bacterial burden and downregulated expression of tissue healing and anti-
439 inflammatory associated genes in comparison to the control group. *Plxdc2*, together with its
440 homologue gene *Plxdc1*, has been identified as one of the membrane receptors of pigment epithelial-
441 derived factor (PEDF) (Cheng et al., 2014), a strong, endogenous anti-angiogenesis factor (Dawson
442 et al., 1999). Interestingly, PEDF treatment modulates macrophage activation in Raw 264.6 cells
443 through the increase of IL-10 production with potential association with PPARγ activation (Yang,
444 Chen, Wu, Ho, & Tsao, 2010; Zamiri, Masli, Streilein, & Taylor, 2006). Cheng et al., reported that
445 PEDF-induced IL-10 production in Raw 264.7 macrophages is dependent on both Plxdc1 and Plxdc2
446 (Cheng et al., 2014). Our data suggest that *Plxdc2* can induce immunological changes independently
447 of the presence of PEDF in addition to in response to PEDF stimulation. The changes observed in
448 the dynamics of *Plxdc2* over the time course and after silencing of the gene suggest additional yet to
449 be discovered signaling mechanisms with impact on anti-bacterial and overall immune responses. As
450 a cell surface receptor, Plxdc2 is a promising therapeutic target for autoimmune diseases.
451
452 The established regulatory effect of PEDF in macrophages, together with the ability to perform ligand-
453 induced activation in addition to the loss of function analysis, triggered the selection of *Plxdc2* for

454 further validation in this initial study. However, the kinetics of *Ppp1r3e* in the validation studies, support
455 the regulatory role of this gene and encourage its further investigation. *Ppp1r3e* gene encodes a
456 glycogen-targeting subunit of the protein serine/threonine phosphatase of type 1 (PP1), a
457 phosphatase protein involved in the regulation of several cell functions, including gene expression,
458 metabolism and cell death (Ceulemans, Stalmans, & Bollen, 2002; Munro, Ceulemans, Bollen,
459 Diplexcito, & Cohen, 2005). Metabolism is an essential component of the immune response (Leber
460 et al., 2017). Activated cells, including macrophages and dendritic cells, undergo metabolic
461 reprogramming, in which glucose metabolism is increased while oxygen consumption is suppressed,
462 to produce energy at fast speed and initiate the mechanisms required for their activation (Kelly &
463 O'Neill, 2015; Rodriguez-Prados et al., 2010). Glycogen-driving subunits, such as *Ppp1r3e*, increase
464 glycogen production promoting glycogen synthase activity (Ceulemans et al., 2002). Moreover,
465 *Ppp1r3e* expression levels are regulated by insulin and are subjected to a significant suppression in
466 diabetic liver (Munro et al., 2005). Interestingly, glycogen also plays a role in the immunometabolic
467 interplay of immune cells (Thwe et al., 2017). Dendritic cells have pools of stored glycogen that is
468 catabolized during the metabolic shift to increase glucose availability and supply the energy needs
469 during these initial steps of the immune response (Thwe et al., 2017). Moreover, deficiencies in
470 glycogen metabolism alter the proper activation of dendritic cells (Thwe et al., 2017). Others have
471 demonstrated that in activated macrophages with overexpression of the glucose transporter GLUT1
472 and increased glucose consumption, glycogen synthesis is upregulated (Freemerman et al., 2014).
473 Therefore, through the modulation of glycogen metabolism, *Ppp1r3e* might modulate the activation of
474 immune cells, and as a consequence, exert important functions associated with the shape of the
475 immune response.
476
477 This study has identified five candidate therapeutic targets with promising host regulatory and
478 immunometabolic roles. Validation studies supported *Plxdc2* and *Ppp1r3e* as two genes with strong
479 regulatory functions and great potential to modulate immune and host responses. Our screening
480 platform can provide new insights in the identification of novel therapeutic targets for the modulation

of the immune response that can drive the next wave of the first-in-class therapeutics for widespread and debilitating autoimmune diseases.

Materials and Methods

Animal housing and ethic statement

C57Bl/6J wild-type (WT) and PPARγfl/fl;LysCre+ (LysCre+) mice were used for these studies. Mice were gender and age-paired between groups to avoid any external variability. Group allocation was randomly performed. Sample-size estimation was performed using the resource equation approach. LysCre+ were generated by breeding of PPARγ fl/fl into Lys-Cre mice, to produce animals lacking PPARγ in myeloid cells. All mice were bred and housed in the same colony at Virginia Tech in ventilated racks and under a 12-hour light cycle. All experimental procedures performed were approved by the Institutional Animal Care and Use Committee (IACUC) and met or exceeded requirements of the Public Health Service/National Institutes of Health and Animal Welfare Act.

Bone marrow-derived macrophages (BMDM) isolation and culture

Bone marrow-derived macrophages (BMDM) were isolated as previously described (Zhang, Goncalves, & Mosser, 2008). Briefly, the femur and tibia were excised, cleaned from the attached muscle and sterilized with 70% ethanol. The distal ends of the bones were cut and the bone marrow (BM) flushed out with cold cRPMI_M, containing RPMI 1640 (Corning Incorporated, Corning, NY), 10% Fetal Bovine Serum (Corning Incorporated, Corning, NY), 2.5% Hepes (Corning Incorporated, Corning, NY), 1% Sodium pyruvate (Corning Incorporated, Corning, NY), 1% L-glutamine (Corning Incorporated, Corning, NY), 1% Penicilin/Streptamicin (Corning Incorporated, Corning, NY) and 50uM β-mercaptoethanol (Sigma Aldrich, St. Louis, MO). Osmotic lysis was used to remove red blood cells. Samples were adjusted to $7.5x10^5$ cells/mL with cold cRPMI_M supplemented with 25 ng/mL of recombinant mouse colony-stimulating factor (m-csf, Peprotech, Rocky Hill, NJ) and cultured at 37ºC, 5% CO_2 and 95% humidity to allow their differentiation. At day 3 fresh m-csf-supplemented media

508 was added. On day 6, plates were washed to remove non-adherent cells and BMDM were harvested.
509 Cells were re-suspended in cRPMI_M and seeded in triplicate in 12-well plates ($5x10^5$ cells per well).
510 Cells were left to adhere overnight at 37ºC, 5% CO_2 and 95% humidity.
511
512 ***H. pylori* culture and preparation of the inoculum**
513 This study was performed using *H. pylori* SS1 strain. *H. pylori* was cultured at 37ºC under
514 microaerophilic conditions in Difco Columbia blood agar (BD Biosciences, San Jose, CA) plates
515 supplemented with 7% of Horse laked blood (Lampire Biological Laboratories, Pipersville, PA) and *H.*
516 *pylori* selective supplement (5mg of Vancomycin, 2.5mg of Trimethoprim, 2.5mg of Cefsulodin and
517 2.5mg of Amphotericin B, Oxoid, Altrincham, England).
518
519 For *in vivo* inoculum preparation, *H. pylori* was harvested at room temperature sterile 1X PBS and
520 adjusted to $2.5x10^8$ colony forming units (cfu) per mL. To obtain the desired concentration, *H. pylori*
521 was adjusted to an optimal density (OD) of 1.2 at a 600-nm wavelength. The association of OD and
522 cfu/mL was based on a previous growth curve that correlated OD with *H. pylori* colony counts. For *in*
523 *vitro* inoculum preparation, *H. pylori* was harvested in antibiotic-free cRPMI and adjusted to $1x10^8$
524 cfu/mL as described above.
525
526 **Gentamycin protection assay**
527 BMDM cells were washed with 1X PBS and fresh antibiotic-free cRPMI was added to the plates. Cells
528 were infected with *H. pylori* SS1 at a MOI 10 and synchronized by a quick spin to ensure immediate
529 contact. After a 15-minute incubation, non-internalized bacteria were killed by thoroughly washing the
530 cells with PBS/5% FBS containing 100ng/ml Gentamycin (Fisher Scientific, Pittsburg, PA). Cells for
531 time-point 0 were washed with PBS and immediately collected for downstream assays. The cells
532 allocated for the remaining time points (30 min to 12 hours) were covered with culture media until
533 collection for bacterial re-isolation or assessment of differential gene expression by qRT-PCR and
534 whole transcriptome analyses. Each validation study included between two and five biological
535 replicates and was repeated at least twice.

536

537 **Bacterial Re-isolation from BMDM**

538 BMDM cells were washed 3 times with sterile 1X PBS. 200uL of Brucella broth (BD Biosciences, San
539 Jose, CA) were added to the well and cells were detached using a cell scraper. Cell suspensions
540 were sonicated 5 seconds to release intracellular bacteria. Serial 10-fold dilutions of the original
541 homogenate were plated into the *H. pylori* plates described above. After for 4 days of culture at 37ºC
542 under microaerophilic conditions, colonies were counted.

543

544 **Gene Expression**

545 BMDM cells were collected in ice-cold RLT (supplemented with β-mercaptoethanol) and stored at -
546 80ºC until RNA isolation was performed. Following mouse euthanasia, stomachs were excised from
547 the animal and longitudinally opened. Collected tissues were rinsed twice in 1X PBS and stored in
548 350uL of RNAlater (Fisher Scientific, Pittsburg, PA) at -80ºC. Total RNA was extracted from BMDM
549 and stomach using the RNeasy mini kit (Qiagen, Hilden, Germany) following manufacturer's
550 instructions. RNA concentrations were quantified with a nandrop (Invitrogen, Carlsbad, CA) at 260nm.
551 iScript cDNA synthesis kit (Bio-Rad, Hercules, CA) was utilized to generate cDNA from RNA samples.
552 Primer-specific amplicons were produced by PCR using Taq Polymerase (Promega, Madison, WI),
553 followed by a purification step using the Mini-Elute PCR purification kit (Qiagen, Hilden, Germany).
554 Standard curves were generated by a series of dilutions from a known concentration of the purified
555 primer-specific amplicon, starting at $1x10^6$pg. Total gene expression levels were assessed through a
556 quantitative real-time PCR (qRT-PCR) using a CFX96 Thermal Cycler (Bio-Rad, Hercules, CA) and
557 SYBR Green Supermix (Bio-Rad, Hercules, CA). βeta-actin expression was utilized to normalize the
558 expression levels of targeted genes. Primer sequences are included in supplementary information.

559

560 **Global Transcriptome analysis**

561 RNA isolated from WT and LysCre+ BMDM collected at time-points 0, 30, 60, 120, 240, 360 and 720
562 minutes post-infection was submitted for whole transcriptome gene expression analysis using Illumina
563 Hiseq (Biocomplexity Institute of Virginia Tech Core Lab Facilities). The biological replicates for each

sample were three. A replicate for three of the samples (LysCre+ HP 0 minutes, LysCre+ HP 120 minutes and WT uninfected 240 minutes) did not pass quality control, therefore these three samples consisted of 2 biological replicates. Once fastq files containing 100bp-long pair-end reads were received, poor quality reads (>40% of bases with PHRED score <10; percentage of N greater than 5%; and polyA reads) were excluded. Through the utilization of Bowtie (Langmead, Trapnell, Pop, & Salzberg, 2009) (version: 1.0.0) with parameters set to '-l 25 -I 1 -X 1000 -a -m 200', the remaining reads we mapped to RefSeq (mm10 from http://genome.ucsc.edu/). To calculate gene expression levels we used RSEM (Li & Dewey, 2011), a program based on expectation-maximization algorithm. FPKM (Trapnell et al., 2010) (fragments per kilobase per million sequenced reads) was used as the measurement of expression level. Data were submitted to NCBI's GEO database (Accession Number GSE67270).

Bioinformatics analysis

As described in **Figure 3C**, to analyze the RNAseq data, an initial dataset of genes linked to the selected NLR and PPAR candidates was generated. Briefly, the Genome-scale Integrated Analysis of gene Networks in Tissues (GIANT) and Gene Expression Omnibus (GEO) databases were used and integrated in the Ingenuity Pathway Analysis (IPA) software to build the initial group of genes. Hierarchical based clustering was employed to obtain differentially expressed patterns within the combined initial NLR and PPAR genes and the linked dataset generated. The *hclust* method with Ward's minimum variance method and Manhattan distance metric in R were used to cluster the data. Another clustering cycle was performed in order to obtain a larger set of genes with similar patterns of interest. The generated dataset was enhanced for novelty through an abstract searching using the Pubmatrix tool, and a final dataset of genes was obtained.

Gene silencing and BMDM treatments

For gene silencing studies, WT and LysCre+ BMDM were transfected with 20nM siRNA (27mer Dicer-substrate siRNA, DsiRNA, for the targeted gene or scrambled sequence as a negative control, Integrated Device Technology, San Jose, CA) using Lipofectamine RNAiMax Transfection Reagent

592 (Thermo Fisher Scientific, Waltham, WA) 48 hours before the infection. Media was replaced 6 hours
593 post-transfection. Cells were exposed to *H. pylori* following the gentamycin protection assay
594 described above. Gene knock-down was validated by qRT-PCR.
595
596 For the induction of a pro-inflammatory environment during gentamycin protection assay, BMDM were
597 pre-treated with LPS (100ng/mL, Sigma Aldrich, St. Louis, MO) and rIFNγ (100ng/mL) overnight. For
598 the LPS validation, BMDM were treated with LPS (100ng/mL) for 1, 2, 4, 6 and 12 hours. For Plxdc2
599 activation, 48 hours post siRNA transfection, WT and LysCre+ BMDM were treated with PEDF (10nM)
600 for 24hours. Then, BMDM were subjected to gentamycin protection assay.
601
602 ***In vivo H. pylori* infection**
603 8 to 12-week-old WT and LysCre+ mice were transferred to an ABSL2 room in the same colony at
604 Virginia Tech in a ventilated rack and under a 12-hour light cycle. On days 0 and 2 of the project, mice
605 were administered 200uL of freshly prepared $5x10^7$ cfu of *H. pylori* SS1 in 1X PBS through orogastric
606 gavage. These studies also included a non-infected group administered with 200uL of 1X PBS without
607 bacteria. Mice were monitored for signs of disease weekly and stomach samples were collected at
608 28 days post-infection.
609
610 **Statistics**
611 Data are expressed as mean values and standard error of the mean represented in error bars. To
612 calculate the significance of the RNAseq dataset from the global transcriptome analysis, all genes
613 with median expression level in all samples greater than 0 were included in a 3-way (genotype,
614 treatment and time) ANOVA analysis. Normal quantile transformation (qqnorm from R (Ihaka &
615 Gentleman, 1996)) was used to normalize the FPKM to fit the normality assumption of ANOVA (tested
616 with Kolmogorov-Smirnov test). The 3-way ANOVA analysis was carried in R (Ihaka & Gentleman,
617 1996), FDR (Benjamini & Hochberg, 1995) and Bonferroni were used to calculate the adjusted *P*-
618 values. To determine significance of the standard data, Analysis of variance (ANOVA) was performed
619 using the general linear model procedure in SAS (SAS Institute). Significance was considered at

620 $p \leq 0.05$ and significant differences were identified with an asterisk (genotype) or pound sign (infection
621 or treatment).
622
623 ## Legends of Primary Figures and Tables
624
625 **Figure 1**. ***Helicobacter pylori* (*H. pylori*) co-culture strongly alters macrophage transcriptomic profile,**
626 **leading to the activation of early regulatory responses and increasing bacterial persistence in WT cells.**
627 WT and PPARγ-deficient (LysCre+) BMDM were co-cultured *ex vivo* with *H. pylori* and cells were harvested at
628 several time-points ranging from 0 to 720 minutes after gentamycin treatment. Bacterial burden (**A**) and gene
629 expression, including IL-10 (**E**) and IFNγ (**F**) were assessed. Differential gene expression based on genotype
630 (**C**) and *H. pylori* infection (**D**) from a whole transcriptomic analysis performed on the harvested cells were also
631 assessed. To classically activate macrophages prior to *H. pylori* co-culture, cells were stimulated with LPS and
632 IFNγ, then challenged with *H. pylori* and the bacterial burden was measured (**B**). **P*-value<0.05 between
633 genotypes, #*P*-value<0.05 within each genotype compared to time 0.
634
635 **Figure 2. Initial analysis and validation of the whole transcriptomic analysis revealed two genes with**
636 **differential expression pattern and well-defined anti-microbial functions.** Plots represent RNAseq reads
637 of *Chil1* (**A**), *Iigp1* (**B**), and *Sqle* (**C**) during the entire time-course comparing genotypes and treatments. *Chil1*
638 (**D**), *Iigp1* (**E**), and *Sqle* (**F**) gene expression from the same co-culture was validated through qRT-PCR. Bacterial
639 loads (**G**) were measured 120 minutes post-gentamycin treatment of *H. pylori* co-cultures in WT and LysCre+
640 macrophages transfected with *Chil1*-targeted, *Iigp1*-targeted or *Sqle*-targeted siRNA or a scrambled sequence
641 as a negative control. **P*-value<0.05 between genotypes, #*P*-value<0.05 within each genotype compared to
642 time 0.
643
644 **Figure 3. Bioinformatics pipeline utilized to analyze the RNAseq dataset and establish the differential**
645 **expression patterns that lead to the identification of the potential regulatory candidates.** Heatmaps
646 represent the genotype fold-change expression from each gene in the NLR (**A**) and PPAR (**D**) pathways. Blue
647 represents inhibited expression in WT macrophages compared to the upregulation in LysCre+, while red
648 indicates upregulation in WT compared to a suppressed expression in LysCre+ macrophages. NLR (**B**) and

649 PPAR (**E**) pathways are represented in this diagram. In red are highlighted the top genes, based on the
650 differential expression analysis represented in the heatmap, and selected as seed genes. Schematic
651 representation of the steps performed during the bioinformatics analysis, after seed genes selection (**C**). The
652 21 genes included in the final set were classified in five groups based on their expression pattern (**F**).
653
654 **Figure 4. Expression kinetics of the five candidates selected from the bioinformatics analysis to**
655 **undergo experimental validation.** *Plxdc2* (**A**), *Ppp1r3e* (**B**), *Vsig8* (**C**), *Ankrd29* (**D**), and *C1qtnf1* (**E**) RNAseq
656 reads in WT and LysCre+ macrophages expressed as FPKM values.
657
658 **Table 1. Gene information and properties of the five top selected candidates.**
659
660 **Figure 5**. ***In vivo* and *in vitro* validation of the five selected candidates under *Helicobacter pylori*-induced**
661 **regulatory conditions.** WT and LysCre+ BMDM were co-cultured *ex vivo* with *H. pylori* and harvested at
662 several time-points ranging from 0 to 720 minutes. *Plxdc2* (**A**), *Ppp1r3e* (**C**), *Vsig8* (**E**), *Ankrd29* (**G**), and *C1qtnf1*
663 (**I**) gene expression was measured by qRT-PCR. WT and LysCre+ mice were infected with *H. pylori* SS1 strain.
664 Non-infected mice were used as control. *Plxdc2* (**B**), *Ppp1r3e* (**D**), *Vsig8* (**F**), *Ankrd29* (**H**) and *C1qtnf1* (**J**) gene
665 expression was measured by qRT-PCR. **P*-value<0.05 between genotypes, #*P*-value<0.05 within each
666 genotype compared to time 0. For in vivo experiments, n=4.
667
668 **Figure 6**. ***In vitro* validation of the five selected candidates under pro-inflammatory conditions.** WT and
669 LysCre+ BMDM were stimulated with 100 ng/ml LPS and harvested at several time points ranging from 0 to
670 720 minutes. *Plxdc2* (**A**), *Ppp1r3e* (**B**), *Vsig8* (**C**), *Ankrd29* (**D**), *C1qtnf1* (**E**), *TNFα* (**F**), *Pparγ* (**G**), and *IL-10* (**H**)
671 gene expression was measured through qRT-PCR. **P*-value<0.05 between genotypes, #*P*-value<0.05 within
672 each genotype compared to time 0.
673
674 **Figure 7**. **Gene silencing and ligand-induced activation studies to confirm the regulatory role of *Plxdc2.***
675 WT and LysCre+ BMDM were transfected with *Plxdc2* or scrambled siRNA as a negative control prior to *H.*
676 *pylori* co-culture *in vitro*. Cells were harvested at 0, 60, 120, 240 and 360 minutes post *H. pylori* challenge and
677 *Plxdc2* (**A**)*, Arg1* (**B**), and *Retnla* (**C**) gene expression was measured. Bacterial burden (**D**) was assessed 120
678 minutes post co-culture. WT and LysCre+ BMDM transfected with *Plxdc2* or scrambled siRNA as a negative

679 control were treated with the Plxdc2 ligand PEDF at 10nM prior to *H. pylori* challenge. At 120 minutes post co-
680 culture cells were harvested, and Arg1 (**E**) and Retnla (**F**) gene expression was assessed. **P*-value<0.05
681 between genotypes, #*P*-value<0.05 within treatment.
682
683 ## Legends of Figure Supplements
684
685 **Figure 2 – figure supplement 1. Expression kinetics of several pro-inflammatory genes during**
686 ***Helicobacter pylori* co-culture.** Plots represent the RNAseq reads comparing WT and LysCre+ BMDM in the
687 distinctive time points of the gentamycin protection assay of *MCP1* (**A**), *MCP5* (**B**), *IL6* (**C**), *IFNγ* (**D**), *IL12a* (**E**),
688 *IL12b* (**F**), *CXCL1* (**G**), *CXCL10* (**H**), and *MIP-1α* (**I**).
689
690 **Figure 2 – figure supplement 2. 3-way ANOVA analyses revealed eight genes with significant differential**
691 **expression pattern.** Plots represent the RNAseq values of *Chil1* (**A**), *Etv5* (**B**), *Iigp1* (**C**), *Ptger4* (**D**), *Sqle* (**E**),
692 *Osm* (**F**), *Rptoros* (**G**), and *Hspa2* (**H**). *P*-value<0.05.
693
694 **Figure 2 – figure supplement 3. Validation of *Chil1* and *Iigp1* gene silencing by qRT-PCR.** WT and LysCre+
695 macrophages were transfected with *Chil1*-targeted, *Iigp1*-targeted or negative scrambled siRNA prior to *H.*
696 *pylori* challenge. Cells were harvested 120 minutes after *H. pylori* co-culture. *Chil1* (**A**) and *Iigp1* (**B**) gene
697 expression was assessed. #*P*-value<0.05 within treatments.
698
699 **Figure 3 – figure supplement 1. Final set of genes from the bioinformatics analysis consists of 21**
700 **candidates classified in five groups based on the expression kinetics.** Plots represent the RNAseq reads
701 at each time point of the experiment comparing WT and LysCre+ BMDM. Group 1 (**A**) includes *Ankrd29*, *Plxdc2*,
702 *Vsig8*, *Gm3435*, *Erdr1*, *C1qtnf1*, and *Cald1*. Group 3 (**B**) consists of *Term1*, *Mafb*, *Tank1*, *Casp1*, *Gm11110*,
703 *Pira4*, and *Dusp6*. Group 2 (**C**) only includes *Ppp1r3e*, whereas group 4 (**D**) includes *Btg2* and *Thbs1*. Group 5
704 (**E**) consists of *Pgm2l1*, *Tnfsf13b*, *Gpnmb,* and *Syngr2*.
705
706 ## Supplementary Files
707

708 Supplementary File 1. qRT-PCR primers utilized in this study.

709

710 **Competing interests**

711

712 The authors declare no competing interests.

713 **References**

714

715 Arango Duque, G., & Descoteaux, A. (2014). Macrophage cytokines: involvement in immunity and
716 infectious diseases. *Front Immunol, 5*, 491. doi:10.3389/fimmu.2014.00491

717 Bassaganya-Riera, J., Dominguez-Bello, M. G., Kronsteiner, B., Carbo, A., Lu, P., Viladomiu, M., . . .
718 Hontecillas, R. (2012). Helicobacter pylori colonization ameliorates glucose homeostasis in
719 mice through a PPAR gamma-dependent mechanism. *PLoS One, 7*(11), e50069.
720 doi:10.1371/journal.pone.0050069

721 Becker, K. G., Hosack, D. A., Dennis, G., Jr., Lempicki, R. A., Bright, T. J., Cheadle, C., & Engel, J. (2003).
722 PubMatrix: a tool for multiplex literature mining. *BMC Bioinformatics, 4*, 61.
723 doi:10.1186/1471-2105-4-61

724 Benjamini, Yoav, & Hochberg, Yosef. (1995). Controlling the False Discovery Rate: A Practical and
725 Powerful Approach to Multiple Testing. *Journal of the Royal Statistical Society. Series B*
726 *(Methodological), 57*(1), 289-300.

727 Bhuiyan, T. R., Islam, M. M., Uddin, T., Chowdhury, M. I., Janzon, A., Adamsson, J., . . . Lundgren, A.
728 (2014). Th1 and Th17 responses to Helicobacter pylori in Bangladeshi infants, children and
729 adults. *PLoS One, 9*(4), e93943. doi:10.1371/journal.pone.0093943

730 Carbo, A., Bassaganya-Riera, J., Pedragosa, M., Viladomiu, M., Marathe, M., Eubank, S., . . .
731 Hontecillas, R. (2013). Predictive computational modeling of the mucosal immune responses
732 during Helicobacter pylori infection. *PLoS One, 8*(9), e73365.
733 doi:10.1371/journal.pone.0073365

734 Caruso, R., Fina, D., Paoluzi, O. A., Del Vecchio Blanco, G., Stolfi, C., Rizzo, A., . . . Monteleone, G.
735 (2008). IL-23-mediated regulation of IL-17 production in Helicobacter pylori-infected gastric
736 mucosa. *Eur J Immunol, 38*(2), 470-478. doi:10.1002/eji.200737635

737 Ceulemans, H., Stalmans, W., & Bollen, M. (2002). Regulator-driven functional diversification of
738 protein phosphatase-1 in eukaryotic evolution. *Bioessays, 24*(4), 371-381.
739 doi:10.1002/bies.10069
740 Cheng, G., Zhong, M., Kawaguchi, R., Kassai, M., Al-Ubaidi, M., Deng, J., . . . Sun, H. (2014).
741 Identification of PLXDC1 and PLXDC2 as the transmembrane receptors for the multifunctional
742 factor PEDF. *Elife, 3*, e05401. doi:10.7554/eLife.05401
743 Chionh, Y. T., Ng, G. Z., Ong, L., Arulmuruganar, A., Stent, A., Saeed, M. A., . . . Sutton, P. (2015).
744 Protease-activated receptor 1 suppresses Helicobacter pylori gastritis via the inhibition of
745 macrophage cytokine secretion and interferon regulatory factor 5. *Mucosal Immunol, 8*(1),
746 68-79. doi:10.1038/mi.2014.43
747 Chu, Y. T., Wang, Y. H., Wu, J. J., & Lei, H. Y. (2010). Invasion and multiplication of Helicobacter pylori
748 in gastric epithelial cells and implications for antibiotic resistance. *Infect Immun, 78*(10), 4157-
749 4165. doi:10.1128/IAI.00524-10
750 D'Elios, M. M., Manghetti, M., De Carli, M., Costa, F., Baldari, C. T., Burroni, D., . . . Del Prete, G. (1997).
751 T helper 1 effector cells specific for Helicobacter pylori in the gastric antrum of patients with
752 peptic ulcer disease. *J Immunol, 158*(2), 962-967.
753 Dawson, D. W., Volpert, O. V., Gillis, P., Crawford, S. E., Xu, H., Benedict, W., & Bouck, N. P. (1999).
754 Pigment epithelium-derived factor: a potent inhibitor of angiogenesis. *Science, 285*(5425),
755 245-248.
756 de Martel, C., Llosa, A. E., Farr, S. M., Friedman, G. D., Vogelman, J. H., Orentreich, N., . . . Parsonnet,
757 J. (2005). Helicobacter pylori infection and the risk of development of esophageal
758 adenocarcinoma. *J Infect Dis, 191*(5), 761-767. doi:10.1086/427659

759 Ernst, P. B., & Gold, B. D. (2000). The disease spectrum of Helicobacter pylori: the
760 immunopathogenesis of gastroduodenal ulcer and gastric cancer. *Annu Rev Microbiol, 54*,
761 615-640. doi:10.1146/annurev.micro.54.1.615
762 Freemerman, A. J., Johnson, A. R., Sacks, G. N., Milner, J. J., Kirk, E. L., Troester, M. A., . . . Makowski,
763 L. (2014). Metabolic reprogramming of macrophages: glucose transporter 1 (GLUT1)-
764 mediated glucose metabolism drives a proinflammatory phenotype. *J Biol Chem, 289*(11),
765 7884-7896. doi:10.1074/jbc.M113.522037
766 Gobert, A. P., Verriere, T., Asim, M., Barry, D. P., Piazuelo, M. B., de Sablet, T., . . . Wilson, K. T. (2014).
767 Heme oxygenase-1 dysregulates macrophage polarization and the immune response to
768 Helicobacter pylori. *J Immunol, 193*(6), 3013-3022. doi:10.4049/jimmunol.1401075
769 Gong, J. H., Zhang, M., Modlin, R. L., Linsley, P. S., Iyer, D., Lin, Y., & Barnes, P. F. (1996). Interleukin-
770 10 downregulates Mycobacterium tuberculosis-induced Th1 responses and CTLA-4
771 expression. *Infect Immun, 64*(3), 913-918.
772 Guirado, E., Rajaram, M. V., Chawla, A., Daigle, J., La Perle, K. M., Arnett, E., . . . Schlesinger, L. S.
773 (2018). Deletion of PPARgamma in lung macrophages provides an immunoprotective
774 response against M. tuberculosis infection in mice. *Tuberculosis (Edinb), 111*, 170-177.
775 doi:10.1016/j.tube.2018.06.012
776 He, Y., Hara, H., & Nunez, G. (2016). Mechanism and Regulation of NLRP3 Inflammasome Activation.
777 *Trends Biochem Sci, 41*(12), 1012-1021. doi:10.1016/j.tibs.2016.09.002
778 Hontecillas, R., Horne, W. T., Climent, M., Guri, A. J., Evans, C., Zhang, Y., . . . Bassaganya-Riera, J.
779 (2011). Immunoregulatory mechanisms of macrophage PPAR-gamma in mice with
780 experimental inflammatory bowel disease. *Mucosal Immunol, 4*(3), 304-313.
781 doi:10.1038/mi.2010.75

Hooi, J. K. Y., Lai, W. Y., Ng, W. K., Suen, M. M. Y., Underwood, F. E., Tanyingoh, D., . . . Ng, S. C. (2017). Global Prevalence of Helicobacter pylori Infection: Systematic Review and Meta-Analysis. *Gastroenterology, 153*(2), 420-429. doi:10.1053/j.gastro.2017.04.022

Ihaka, Ross, & Gentleman, Robert. (1996). R: A Language for Data Analysis and Graphics. *Journal of Computational and Graphical Statistics, 5*(3), 299-314. doi:10.1080/10618600.1996.10474713

Imamura, R., Wang, Y., Kinoshita, T., Suzuki, M., Noda, T., Sagara, J., . . . Suda, T. (2010). Anti-inflammatory activity of PYNOD and its mechanism in humans and mice. *J Immunol, 184*(10), 5874-5884. doi:10.4049/jimmunol.0900779

Ip, W. K. E., Hoshi, N., Shouval, D. S., Snapper, S., & Medzhitov, R. (2017). Anti-inflammatory effect of IL-10 mediated by metabolic reprogramming of macrophages. *Science, 356*(6337), 513-519. doi:10.1126/science.aal3535

Jha, A. K., Huang, S. C., Sergushichev, A., Lampropoulou, V., Ivanova, Y., Loginicheva, E., . . . Artyomov, M. N. (2015). Network integration of parallel metabolic and transcriptional data reveals metabolic modules that regulate macrophage polarization. *Immunity, 42*(3), 419-430. doi:10.1016/j.immuni.2015.02.005

Kabisch, R., Semper, R. P., Wustner, S., Gerhard, M., & Mejias-Luque, R. (2016). Helicobacter pylori gamma-Glutamyltranspeptidase Induces Tolerogenic Human Dendritic Cells by Activation of Glutamate Receptors. *J Immunol, 196*(10), 4246-4252. doi:10.4049/jimmunol.1501062

Kaebisch, R., Mejias-Luque, R., Prinz, C., & Gerhard, M. (2014). Helicobacter pylori cytotoxin-associated gene A impairs human dendritic cell maturation and function through IL-10-mediated activation of STAT3. *J Immunol, 192*(1), 316-323. doi:10.4049/jimmunol.1302476

Kawai, T., & Akira, S. (2006). TLR signaling. *Cell Death Differ, 13*(5), 816-825. doi:10.1038/sj.cdd.4401850

Kelly, B., & O'Neill, L. A. (2015). Metabolic reprogramming in macrophages and dendritic cells in innate immunity. *Cell Res, 25*(7), 771-784. doi:10.1038/cr.2015.68

Kim, Y. K., Shin, J. S., & Nahm, M. H. (2016). NOD-Like Receptors in Infection, Immunity, and Diseases. *Yonsei Med J, 57*(1), 5-14. doi:10.3349/ymj.2016.57.1.5

Kusters, J. G., van Vliet, A. H., & Kuipers, E. J. (2006). Pathogenesis of Helicobacter pylori infection. *Clin Microbiol Rev, 19*(3), 449-490. doi:10.1128/CMR.00054-05

Langmead, B., Trapnell, C., Pop, M., & Salzberg, S. L. (2009). Ultrafast and memory-efficient alignment of short DNA sequences to the human genome. *Genome Biol, 10*(3), R25. doi:10.1186/gb-2009-10-3-r25

Leber, A., Bassaganya-Riera, J., Tubau-Juni, N., Zoccoli-Rodriguez, V., Viladomiu, M., Abedi, V., . . . Hontecillas, R. (2016). Modeling the Role of Lanthionine Synthetase C-Like 2 (LANCL2) in the Modulation of Immune Responses to Helicobacter pylori Infection. *PLoS One, 11*(12), e0167440. doi:10.1371/journal.pone.0167440

Leber, A., Hontecillas, R., Tubau-Juni, N., Zoccoli-Rodriguez, V., Abedi, V., & Bassaganya-Riera, J. (2018). NLRX1 Modulates Immunometabolic Mechanisms Controlling the Host-Gut Microbiota Interactions during Inflammatory Bowel Disease. *Front Immunol, 9*, 363. doi:10.3389/fimmu.2018.00363

Leber, A., Hontecillas, R., Tubau-Juni, N., Zoccoli-Rodriguez, V., Hulver, M., McMillan, R., . . . Bassaganya-Riera, J. (2017). NLRX1 Regulates Effector and Metabolic Functions of CD4(+) T Cells. *J Immunol, 198*(6), 2260-2268. doi:10.4049/jimmunol.1601547

Li, B., & Dewey, C. N. (2011). RSEM: accurate transcript quantification from RNA-Seq data with or without a reference genome. *BMC Bioinformatics, 12*, 323. doi:10.1186/1471-2105-12-323

Liu, T., Zhang, L., Joo, D., & Sun, S. C. (2017). NF-kappaB signaling in inflammation. *Signal Transduct Target Ther, 2*. doi:10.1038/sigtrans.2017.23

Lundgren, A., Suri-Payer, E., Enarsson, K., Svennerholm, A. M., & Lundin, B. S. (2003). Helicobacter pylori-specific CD4+ CD25high regulatory T cells suppress memory T-cell responses to H. pylori in infected individuals. *Infect Immun, 71*(4), 1755-1762.

Malur, A., McCoy, A. J., Arce, S., Barna, B. P., Kavuru, M. S., Malur, A. G., & Thomassen, M. J. (2009). Deletion of PPAR gamma in alveolar macrophages is associated with a Th-1 pulmonary inflammatory response. *J Immunol, 182*(9), 5816-5822. doi:10.4049/jimmunol.0803504

Masters, S. L., Gerlic, M., Metcalf, D., Preston, S., Pellegrini, M., O'Donnell, J. A., . . . Croker, B. A. (2012). NLRP1 inflammasome activation induces pyroptosis of hematopoietic progenitor cells. *Immunity, 37*(6), 1009-1023. doi:10.1016/j.immuni.2012.08.027

Miller, S. F., Summerhurst, K., Runker, A. E., Kerjan, G., Friedel, R. H., Chedotal, A., . . . Mitchell, K. J. (2007). Expression of Plxdc2/TEM7R in the developing nervous system of the mouse. *Gene Expr Patterns, 7*(5), 635-644. doi:10.1016/j.modgep.2006.12.002

Miller-Delaney, S. F., Lieberam, I., Murphy, P., & Mitchell, K. J. (2011). Plxdc2 is a mitogen for neural progenitors. *PLoS One, 6*(1), e14565. doi:10.1371/journal.pone.0014565

Moreira-Teixeira, L., Redford, P. S., Stavropoulos, E., Ghilardi, N., Maynard, C. L., Weaver, C. T., . . . O'Garra, A. (2017). T Cell-Derived IL-10 Impairs Host Resistance to Mycobacterium tuberculosis Infection. *J Immunol, 199*(2), 613-623. doi:10.4049/jimmunol.1601340

Munro, S., Ceulemans, H., Bollen, M., Diplexcito, J., & Cohen, P. T. (2005). A novel glycogen-targeting subunit of protein phosphatase 1 that is regulated by insulin and shows differential tissue distribution in humans and rodents. *FEBS J, 272*(6), 1478-1489. doi:10.1111/j.1742-4658.2005.04585.x

Namgaladze, D., Lips, S., Leiker, T. J., Murphy, R. C., Ekroos, K., Ferreiros, N., . . . Brune, B. (2014). Inhibition of macrophage fatty acid beta-oxidation exacerbates palmitate-induced

853 inflammatory and endoplasmic reticulum stress responses. *Diabetologia, 57*(5), 1067-1077.
854 doi:10.1007/s00125-014-3173-4
855 Noto, J. M., & Peek, R. M., Jr. (2017). The gastric microbiome, its interaction with Helicobacter pylori,
856 and its potential role in the progression to stomach cancer. *PLoS Pathog, 13*(10), e1006573.
857 doi:10.1371/journal.ppat.1006573
858 O'Leary, S., O'Sullivan, M. P., & Keane, J. (2011). IL-10 blocks phagosome maturation in
859 mycobacterium tuberculosis-infected human macrophages. *Am J Respir Cell Mol Biol, 45*(1),
860 172-180. doi:10.1165/rcmb.2010-0319OC
861 O'Rourke, J., & Bode, G. (2001). Morphology and Ultrastructure. In H. L. T. Mobley, G. L. Mendz, & S.
862 L. Hazell (Eds.), *Helicobacter pylori: Physiology and Genetics*. Washington (DC).
863 Odegaard, J. I., Ricardo-Gonzalez, R. R., Goforth, M. H., Morel, C. R., Subramanian, V., Mukundan, L.,
864 . . . Chawla, A. (2007). Macrophage-specific PPARgamma controls alternative activation and
865 improves insulin resistance. *Nature, 447*(7148), 1116-1120. doi:10.1038/nature05894
866 Oh, J. D., Karam, S. M., & Gordon, J. I. (2005). Intracellular Helicobacter pylori in gastric epithelial
867 progenitors. *Proc Natl Acad Sci U S A, 102*(14), 5186-5191. doi:10.1073/pnas.0407657102
868 Raghavan, S., Fredriksson, M., Svennerholm, A. M., Holmgren, J., & Suri-Payer, E. (2003). Absence of
869 CD4+CD25+ regulatory T cells is associated with a loss of regulation leading to increased
870 pathology in Helicobacter pylori-infected mice. *Clin Exp Immunol, 132*(3), 393-400.
871 Raghavan, S., & Quiding-Jarbrink, M. (2012). Immune modulation by regulatory T cells in Helicobacter
872 pylori-associated diseases. *Endocr Metab Immune Disord Drug Targets, 12*(1), 71-85.
873 Redford, P. S., Murray, P. J., & O'Garra, A. (2011). The role of IL-10 in immune regulation during M.
874 tuberculosis infection. *Mucosal Immunol, 4*(3), 261-270. doi:10.1038/mi.2011.7

875 Reibman, J., Marmor, M., Filner, J., Fernandez-Beros, M. E., Rogers, L., Perez-Perez, G. I., & Blaser, M.
876 J. (2008). Asthma is inversely associated with Helicobacter pylori status in an urban
877 population. *PLoS One, 3*(12), e4060. doi:10.1371/journal.pone.0004060
878 Rodriguez-Prados, J. C., Traves, P. G., Cuenca, J., Rico, D., Aragones, J., Martin-Sanz, P., . . . Bosca, L.
879 (2010). Substrate fate in activated macrophages: a comparison between innate, classic, and
880 alternative activation. *J Immunol, 185*(1), 605-614. doi:10.4049/jimmunol.0901698
881 Sheh, A., & Fox, J. G. (2013). The role of the gastrointestinal microbiome in Helicobacter pylori
882 pathogenesis. *Gut Microbes, 4*(6), 505-531. doi:10.4161/gmic.26205
883 Shi, Y., Liu, X. F., Zhuang, Y., Zhang, J. Y., Liu, T., Yin, Z., . . . Zou, Q. M. (2010). Helicobacter pylori-
884 induced Th17 responses modulate Th1 cell responses, benefit bacterial growth, and
885 contribute to pathology in mice. *J Immunol, 184*(9), 5121-5129.
886 doi:10.4049/jimmunol.0901115
887 Smythies, L. E., Waites, K. B., Lindsey, J. R., Harris, P. R., Ghiara, P., & Smith, P. D. (2000). Helicobacter
888 pylori-induced mucosal inflammation is Th1 mediated and exacerbated in IL-4, but not IFN-
889 gamma, gene-deficient mice. *J Immunol, 165*(2), 1022-1029.
890 Szanto, A., Balint, B. L., Nagy, Z. S., Barta, E., Dezso, B., Pap, A., . . . Nagy, L. (2010). STAT6 transcription
891 factor is a facilitator of the nuclear receptor PPARgamma-regulated gene expression in
892 macrophages and dendritic cells. *Immunity, 33*(5), 699-712.
893 doi:10.1016/j.immuni.2010.11.009
894 Tanaka, H., Yoshida, M., Nishiumi, S., Ohnishi, N., Kobayashi, K., Yamamoto, K., . . . Azuma, T. (2010).
895 The CagA protein of Helicobacter pylori suppresses the functions of dendritic cell in mice. *Arch*
896 *Biochem Biophys, 498*(1), 35-42. doi:10.1016/j.abb.2010.03.021

Tang, B., Li, N., Gu, J., Zhuang, Y., Li, Q., Wang, H. G., . . . Mao, X. H. (2012). Compromised autophagy by MIR30B benefits the intracellular survival of Helicobacter pylori. *Autophagy, 8*(7), 1045-1057. doi:10.4161/auto.20159

Thwe, P. M., Pelgrom, L., Cooper, R., Beauchamp, S., Reisz, J. A., D'Alessandro, A., . . . Amiel, E. (2017). Cell-Intrinsic Glycogen Metabolism Supports Early Glycolytic Reprogramming Required for Dendritic Cell Immune Responses. *Cell Metab, 26*(3), 558-567 e555. doi:10.1016/j.cmet.2017.08.012

Trapnell, C., Williams, B. A., Pertea, G., Mortazavi, A., Kwan, G., van Baren, M. J., . . . Pachter, L. (2010). Transcript assembly and quantification by RNA-Seq reveals unannotated transcripts and isoform switching during cell differentiation. *Nat Biotechnol, 28*(5), 511-515. doi:10.1038/nbt.1621

van Wijck, Y., de Kleijn, S., John-Schuster, G., Mertens, T. C. J., Hiemstra, P. S., Muller, A., . . . Taube, C. (2018). Therapeutic Application of an Extract of Helicobacter pylori Ameliorates the Development of Allergic Airway Disease. *J Immunol, 200*(5), 1570-1579. doi:10.4049/jimmunol.1700987

Varga, T., Czimmerer, Z., & Nagy, L. (2011). PPARs are a unique set of fatty acid regulated transcription factors controlling both lipid metabolism and inflammation. *Biochim Biophys Acta, 1812*(8), 1007-1022. doi:10.1016/j.bbadis.2011.02.014

Vats, D., Mukundan, L., Odegaard, J. I., Zhang, L., Smith, K. L., Morel, C. R., . . . Chawla, A. (2006). Oxidative metabolism and PGC-1beta attenuate macrophage-mediated inflammation. *Cell Metab, 4*(1), 13-24. doi:10.1016/j.cmet.2006.05.011

Viladomiu, M., Bassaganya-Riera, J., Tubau-Juni, N., Kronsteiner, B., Leber, A., Philipson, C. W., . . . Hontecillas, R. (2017). Cooperation of Gastric Mononuclear Phagocytes with Helicobacter pylori during Colonization. *J Immunol, 198*(8), 3195-3204. doi:10.4049/jimmunol.1601902

921 Viladomiu, M., Hontecillas, R., Pedragosa, M., Carbo, A., Hoops, S., Michalak, P., . . . Bassaganya-Riera,
922 J. (2012). Modeling the role of peroxisome proliferator-activated receptor gamma and
923 microRNA-146 in mucosal immune responses to Clostridium difficile. *PLoS One, 7*(10),
924 e47525. doi:10.1371/journal.pone.0047525
925 Wang, Y. H., Wu, J. J., & Lei, H. Y. (2009). The autophagic induction in Helicobacter pylori-infected
926 macrophage. *Exp Biol Med (Maywood), 234*(2), 171-180. doi:10.3181/0808-RM-252
927 Wroblewski, L. E., Peek, R. M., Jr., & Wilson, K. T. (2010). Helicobacter pylori and gastric cancer:
928 factors that modulate disease risk. *Clin Microbiol Rev, 23*(4), 713-739.
929 doi:10.1128/CMR.00011-10
930 Xia, X., Cui, J., Wang, H. Y., Zhu, L., Matsueda, S., Wang, Q., . . . Wang, R. F. (2011). NLRX1 negatively
931 regulates TLR-induced NF-kappaB signaling by targeting TRAF6 and IKK. *Immunity, 34*(6), 843-
932 853. doi:10.1016/j.immuni.2011.02.022
933 Xie, F. J., Zhang, Y. P., Zheng, Q. Q., Jin, H. C., Wang, F. L., Chen, M., . . . Mao, W. M. (2013).
934 Helicobacter pylori infection and esophageal cancer risk: an updated meta-analysis. *World J*
935 *Gastroenterol, 19*(36), 6098-6107. doi:10.3748/wjg.v19.i36.6098
936 Yang, S. L., Chen, S. L., Wu, J. Y., Ho, T. C., & Tsao, Y. P. (2010). Pigment epithelium-derived factor
937 induces interleukin-10 expression in human macrophages by induction of PPAR gamma. *Life*
938 *Sci, 87*(1-2), 26-35. doi:10.1016/j.lfs.2010.05.007
939 Zamiri, P., Masli, S., Streilein, J. W., & Taylor, A. W. (2006). Pigment epithelial growth factor
940 suppresses inflammation by modulating macrophage activation. *Invest Ophthalmol Vis Sci,*
941 *47*(9), 3912-3918. doi:10.1167/iovs.05-1267
942 Zhang, X., Goncalves, R., & Mosser, D. M. (2008). The isolation and characterization of murine
943 macrophages. *Curr Protoc Immunol, Chapter 14*, Unit 14 11.
944 doi:10.1002/0471142735.im1401s83

945 Zhong, Y., Kinio, A., & Saleh, M. (2013). Functions of NOD-Like Receptors in Human Diseases. *Front*

946 *Immunol, 4*, 333. doi:10.3389/fimmu.2013.00333

947

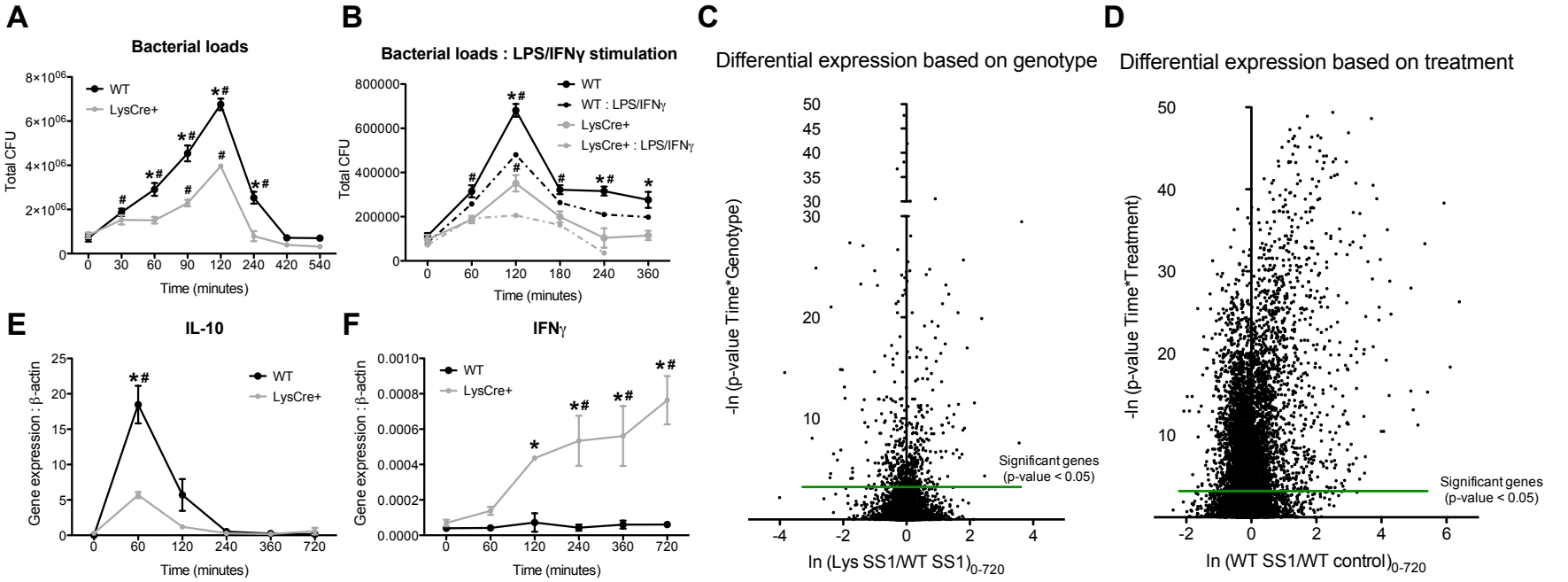
A
Bacterial loads
Total CFU
8×10^06
6×10^06
4×10^06
2×10^06
0
WT
LysCre+
0 30 60 90 120 240 420 540
Time (minutes)
B
Bacterial loads : LPS/IFNγ stimulation
Total CFU
800000
600000
400000
200000
0
WT
WT : LPS/IFNγ
LysCre+
LysCre+ : LPS/IFNγ
0 60 120 180 240 360
Time (minutes)
C
Differential expression based on genotype
-ln (p-value Time*Genotype)
50
45
40
35
30
20
10
Significant genes
(p-value < 0.05)
-4 -2 0 2 4
ln (Lys SS1/WT SS1)0-720
D
Differential expression based on treatment
-ln (p-value Time*Treatment)
50
40
30
20
10
Significant genes
(p-value < 0.05)
-2 0 2 4 6
ln (WT SS1/WT control)0-720
E
IL-10
Gene expression : β-actin
25
20
15
10
5
0
WT
LysCre+
0 60 120 240 360 720
Time (minutes)
F
IFNγ
Gene expression : β-actin
0.0010
0.0008
0.0006
0.0004
0.0002
0.0000
WT
LysCre+
0 60 120 240 360 720
Time (minutes)

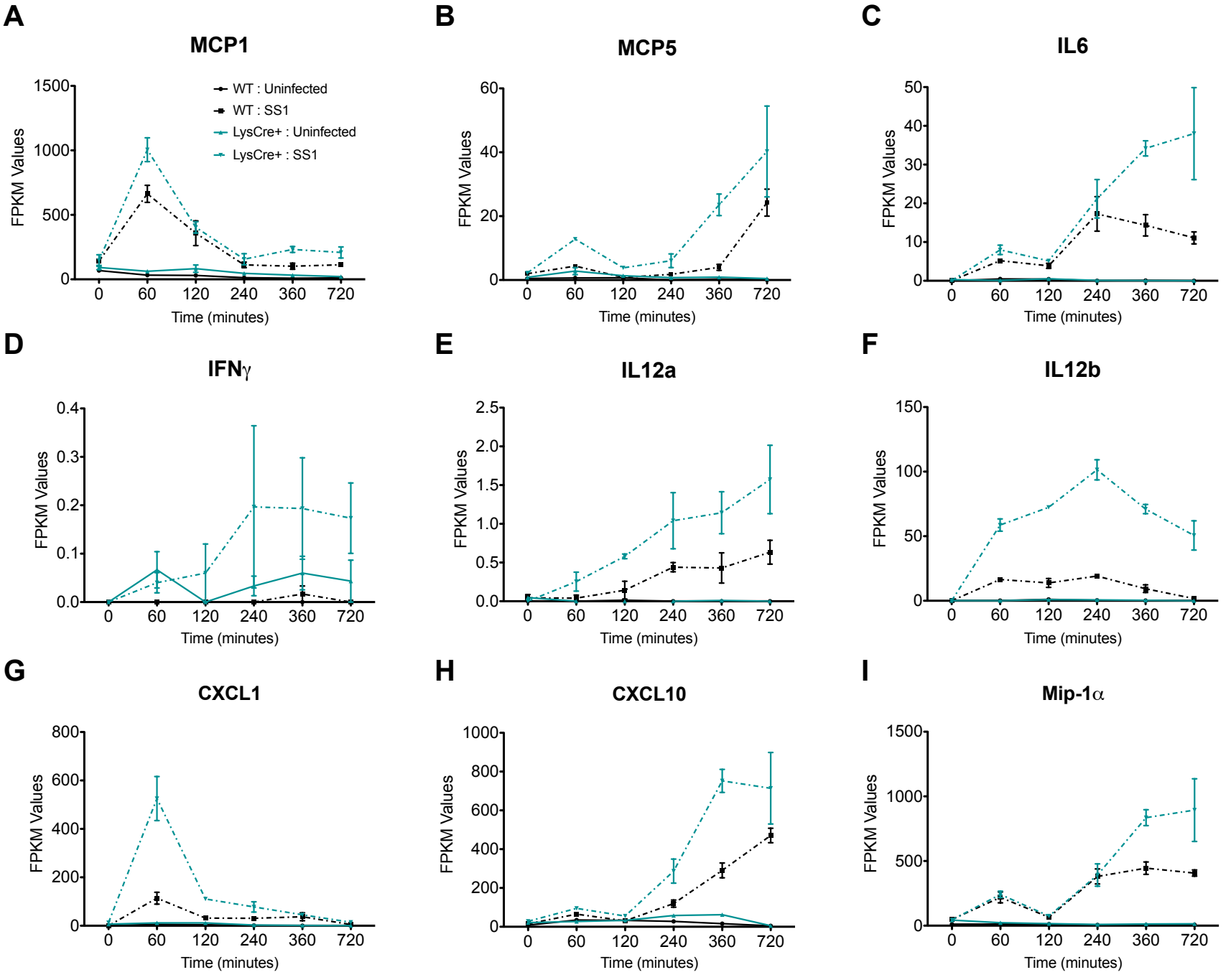
A
MCP1
WT : Uninfected
WT : SS1
LysCre+ : Uninfected
LysCre+ : SS1
FPKM Values
Time (minutes)
B
MCP5
C
IL6
D
IFNγ
E
IL12a
F
IL12b
G
CXCL1
H
CXCL10
I
Mip-1α

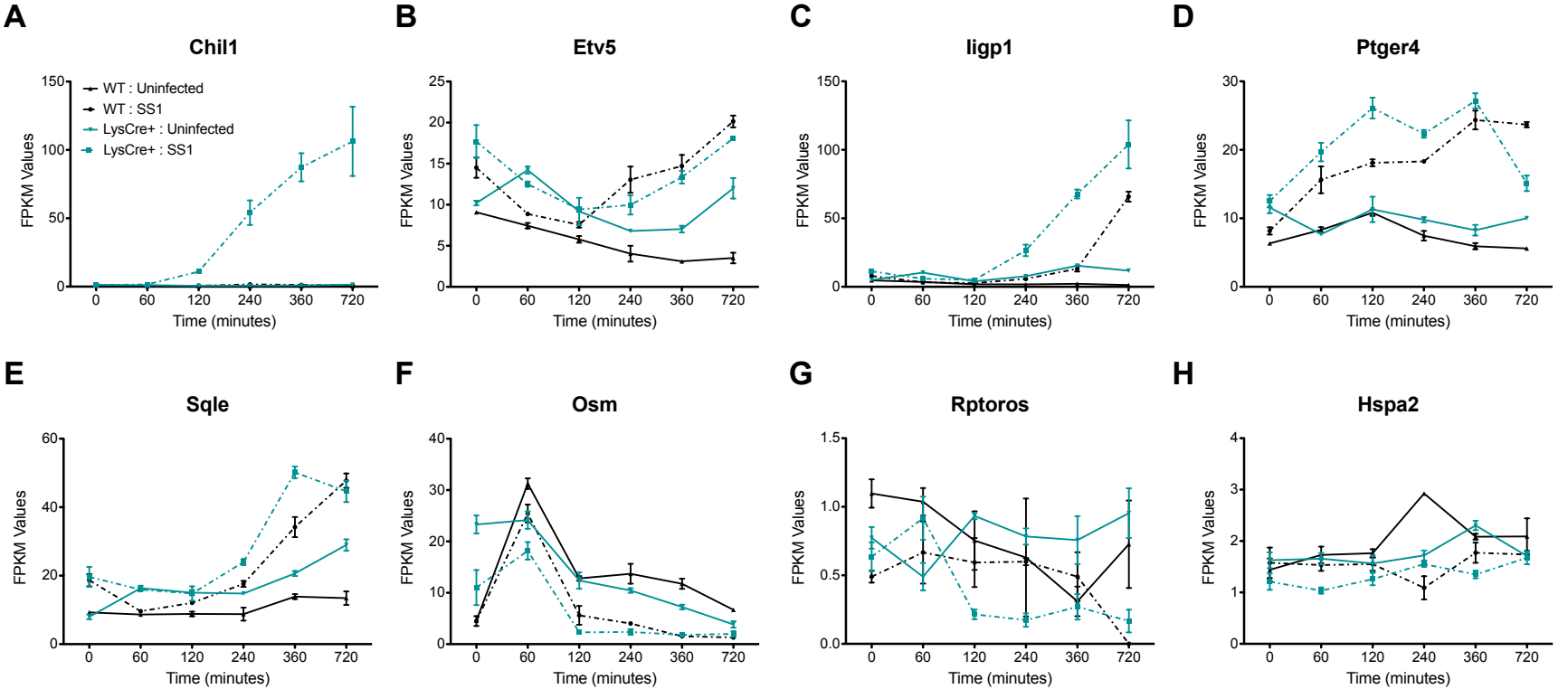
A
Chil1
WT : Uninfected
WT : SS1
LysCre+ : Uninfected
LysCre+ : SS1
FPKM Values
Time (minutes)
B
Etv5
C
Iigp1
D
Ptger4
E
Sqle
F
Osm
G
Rptoros
H
Hspa2

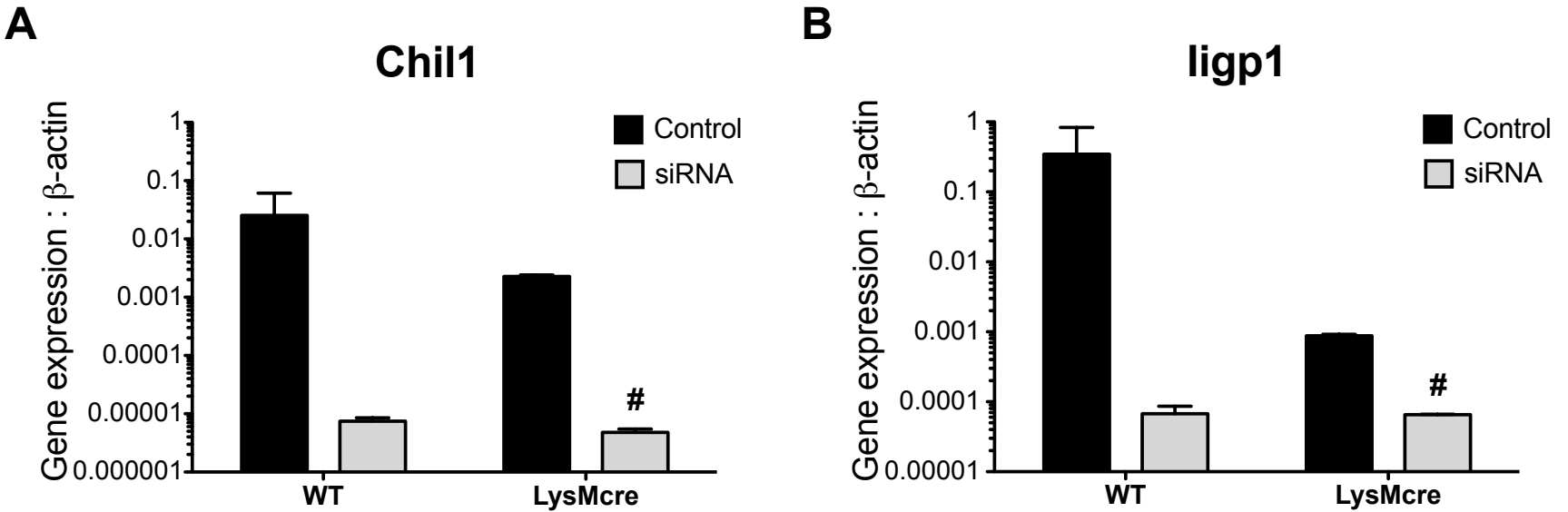
A
Chil1
Gene expression : β-actin
1
0.1
0.01
0.001
0.0001
0.00001
0.000001
Control
siRNA
#
WT
LysMcre
B
Igp1
Gene expression : β-actin
1
0.1
0.01
0.001
0.0001
0.00001
Control
siRNA
#
WT
LysMcre

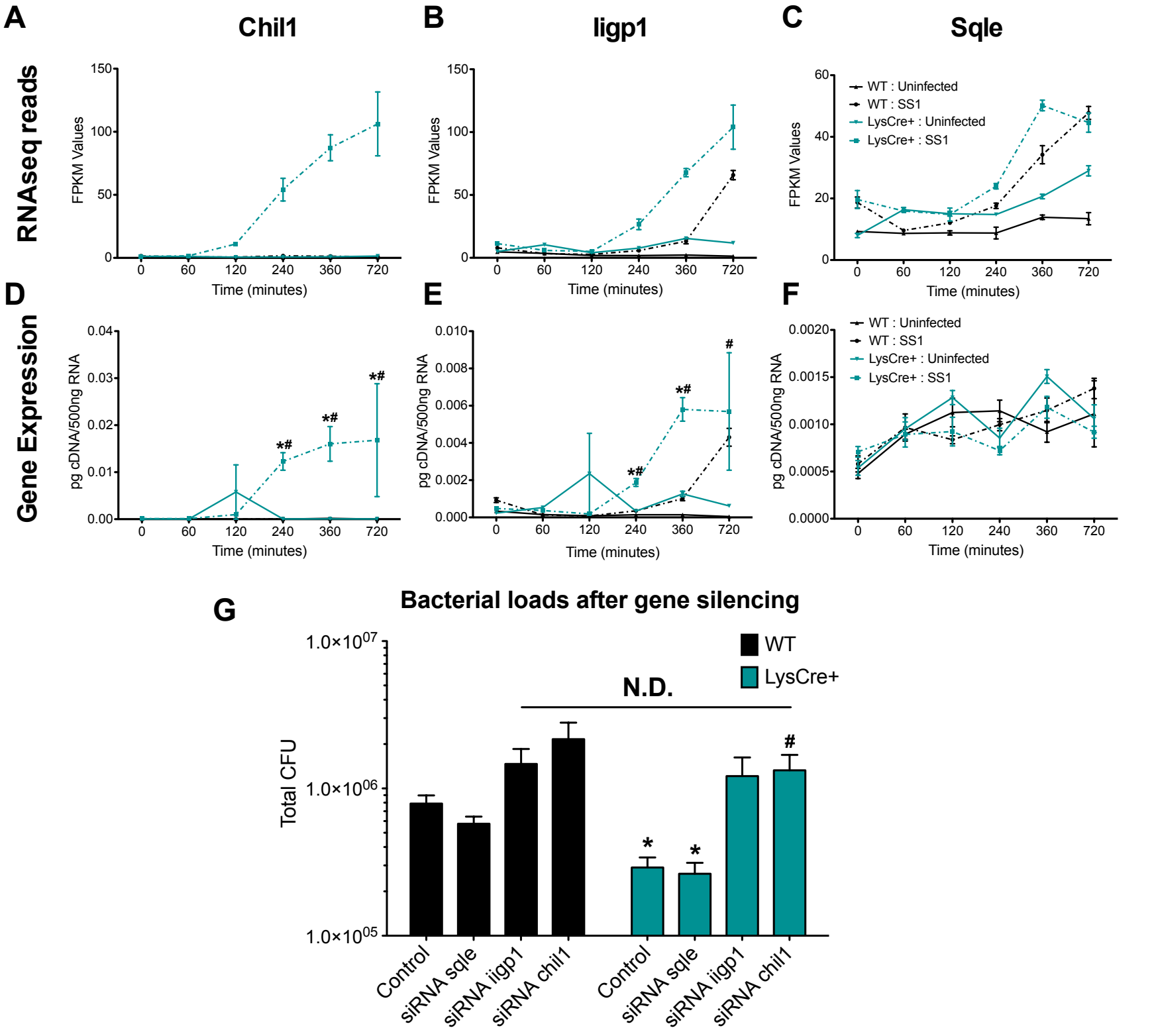
A
Chil1
B
Iigp1
C
Sqle
RNAseq reads
FPKM Values
Time (minutes)
WT : Uninfected
WT : SS1
LysCre+ : Uninfected
LysCre+ : SS1
D
E
F
Gene Expression
pg cDNA/500ng RNA
G
Bacterial loads after gene silencing
WT
LysCre+
N.D.
Total CFU
Control
siRNA sqle
siRNA iigp1
siRNA chil1

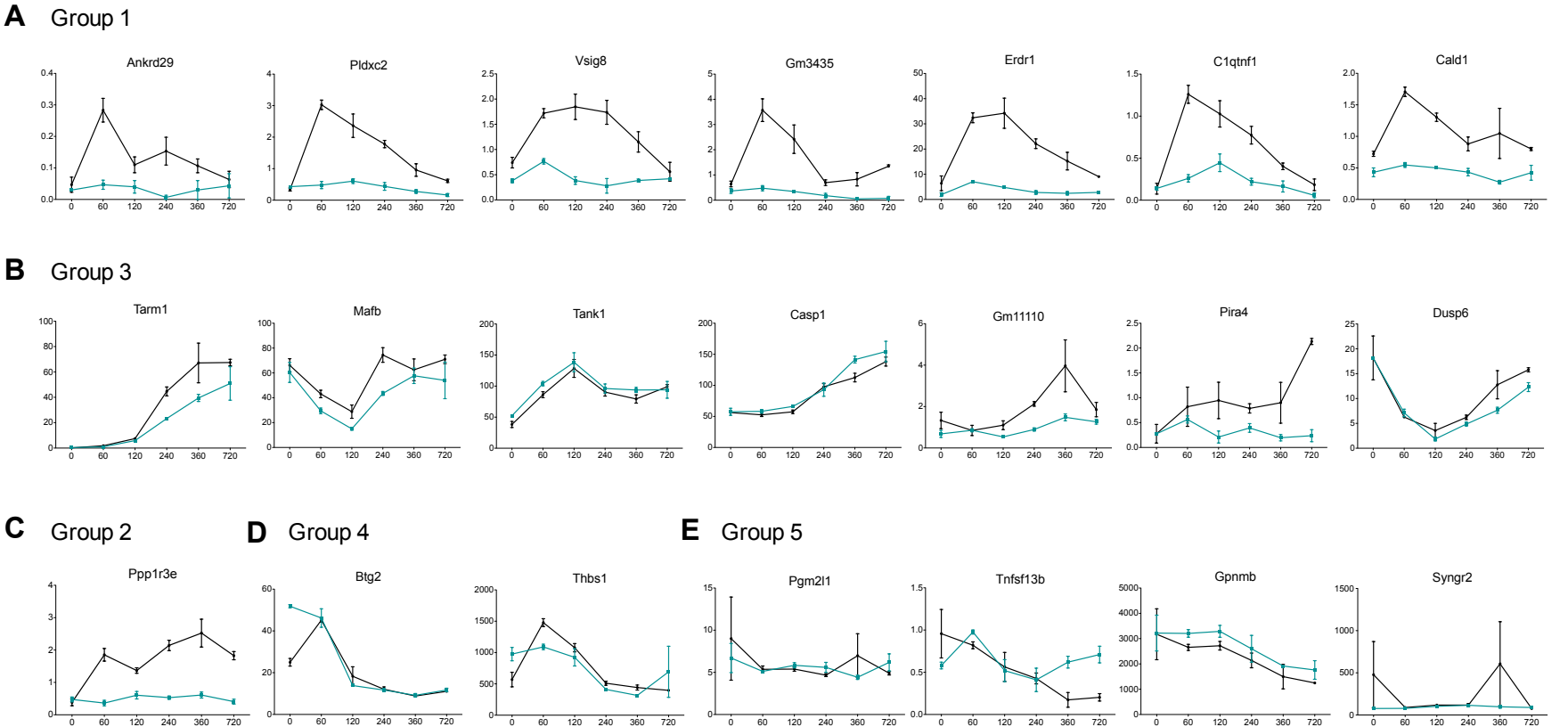
A
Group 1
Ankrd29
Pldxc2
Vsig8
Gm3435
Erdr1
C1qtnf1
Cald1
B
Group 3
Tarm1
Mafb
Tank1
Casp1
Gm11110
Pira4
Dusp6
C
Group 2
Ppp1r3e
D
Group 4
Btg2
Thbs1
E
Group 5
Pgm2l1
Tnfsf13b
Gpnmb
Syngr2

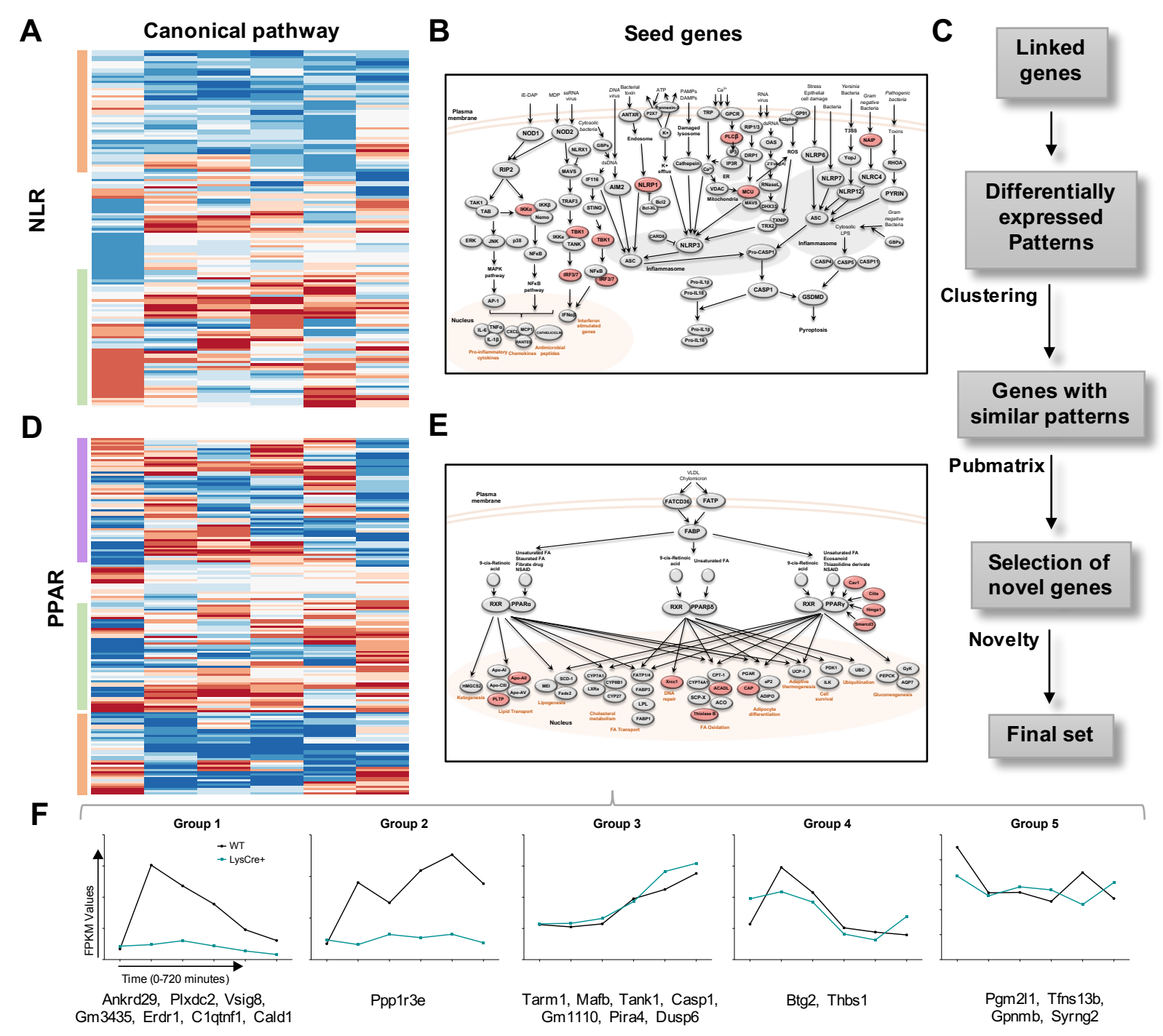
A
Canonical pathway
NLR
B
Seed genes
C
Linked genes
Differentially expressed Patterns
Clustering
Genes with similar patterns
Pubmatrix
Selection of novel genes
Novelty
Final set
D
PPAR
E
F
Group 1
Group 2
Group 3
Group 4
Group 5
WT
LysCre+
FPKM Values
Time (0-720 minutes)
Ankrd29, Plxdc2, Vsig8, Gm3435, Erdr1, C1qtnf1, Cald1
Ppp1r3e
Tarm1, Mafb, Tank1, Casp1, Gm1110, Pira4, Dusp6
Btg2, Thbs1
Pgm2l1, Tfns13b, Gpnmb, Syrng2

A

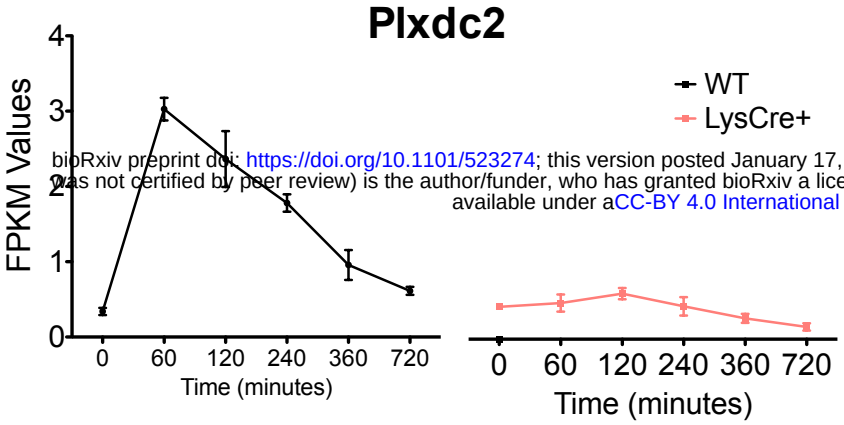

B

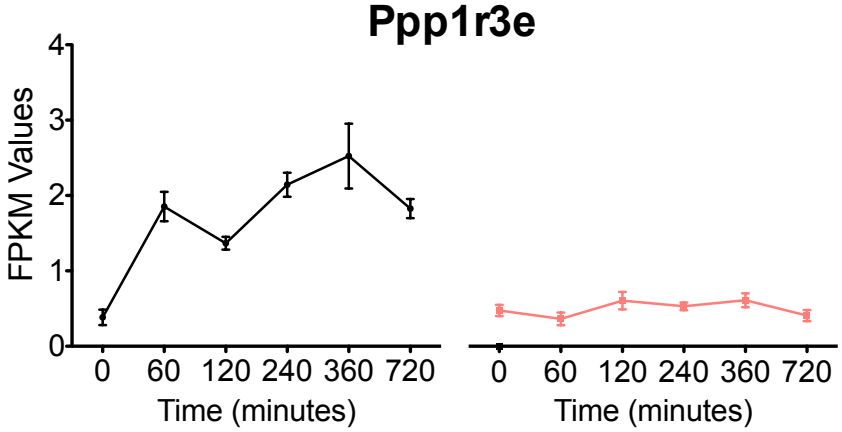

C

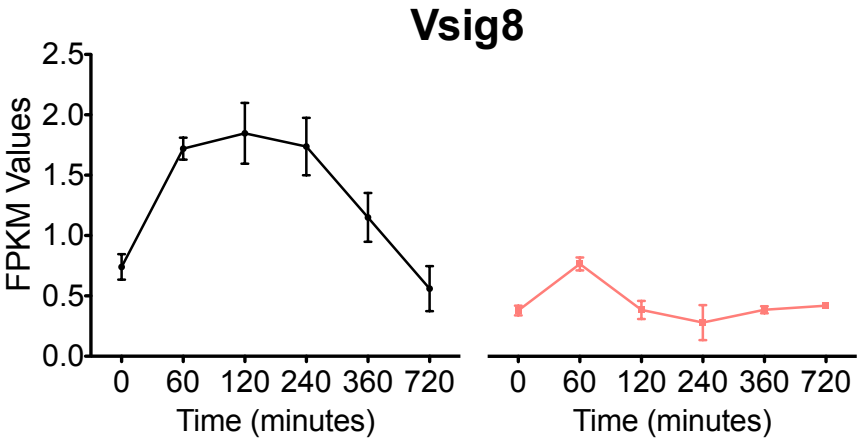

D

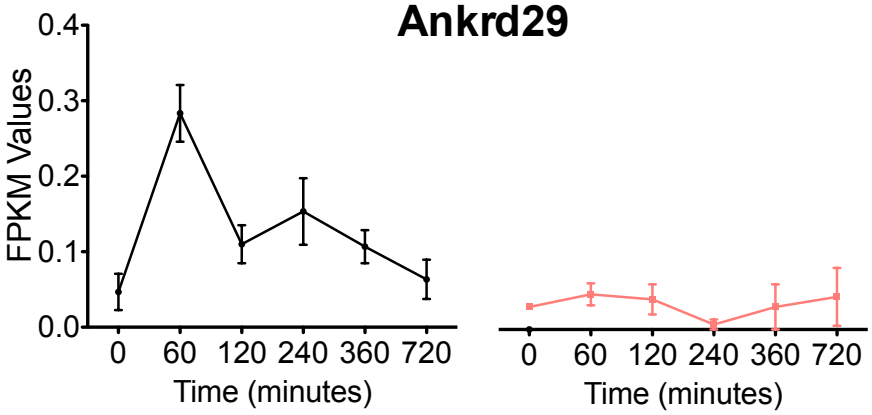

E

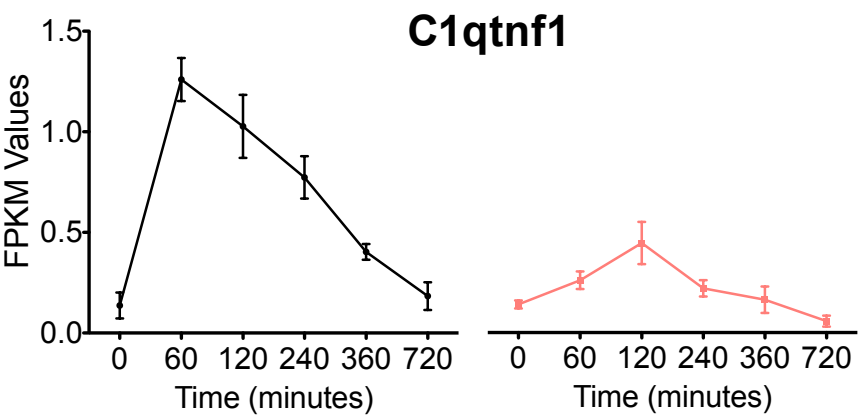

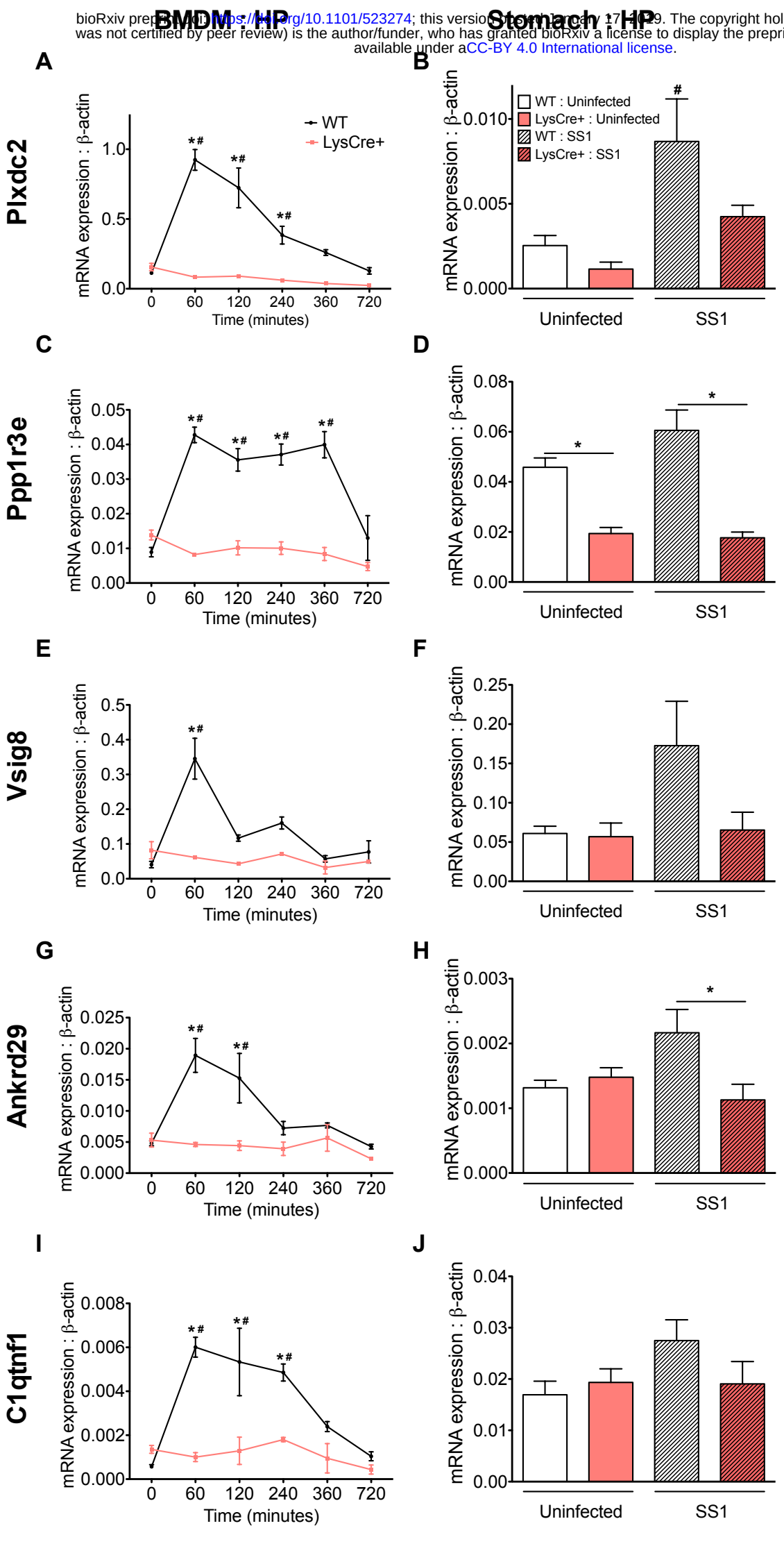

BMDM : LPS

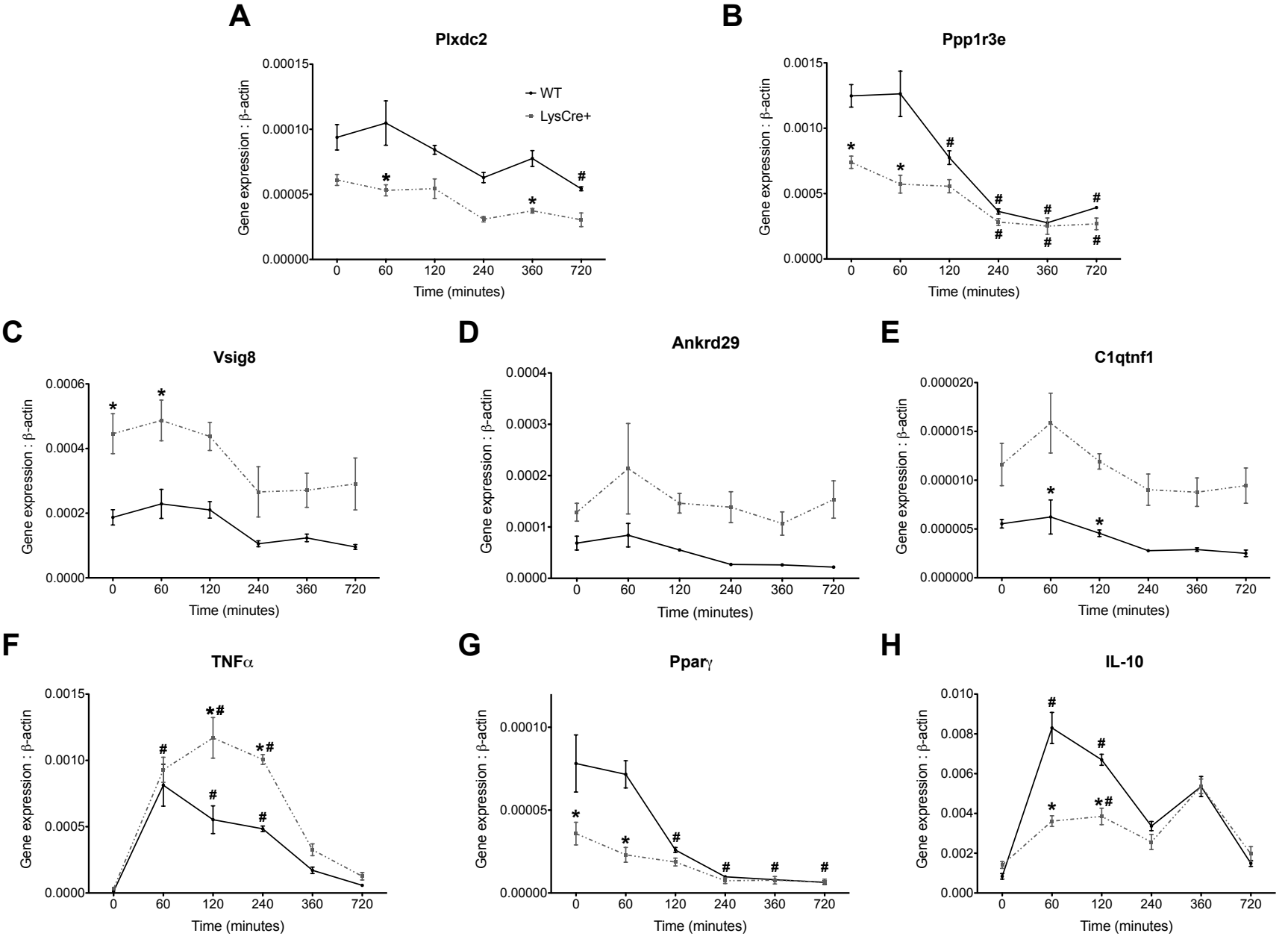
A
Plxdc2
Gene expression : β-actin
0.00015
0.00010
0.00005
0.00000
WT
LysCre+
0 60 120 240 360 720
Time (minutes)
B
Ppp1r3e
Gene expression : β-actin
0.0015
0.0010
0.0005
0.0000
0 60 120 240 360 720
Time (minutes)
C
Vsig8
Gene expression : β-actin
0.0006
0.0004
0.0002
0.0000
0 60 120 240 360 720
Time (minutes)
D
Ankrd29
Gene expression : β-actin
0.0004
0.0003
0.0002
0.0001
0.0000
0 60 120 240 360 720
Time (minutes)
E
C1qtnf1
Gene expression : β-actin
0.000020
0.000015
0.000010
0.000005
0.000000
0 60 120 240 360 720
Time (minutes)
F
TNFα
Gene expression : β-actin
0.0015
0.0010
0.0005
0.0000
0 60 120 240 360 720
Time (minutes)
G
Pparγ
Gene expression : β-actin
0.00010
0.00005
0.00000
0 60 120 240 360 720
Time (minutes)
H
IL-10
Gene expression : β-actin
0.010
0.008
0.006
0.004
0.002
0.000
0 60 120 240 360 720
Time (minutes)

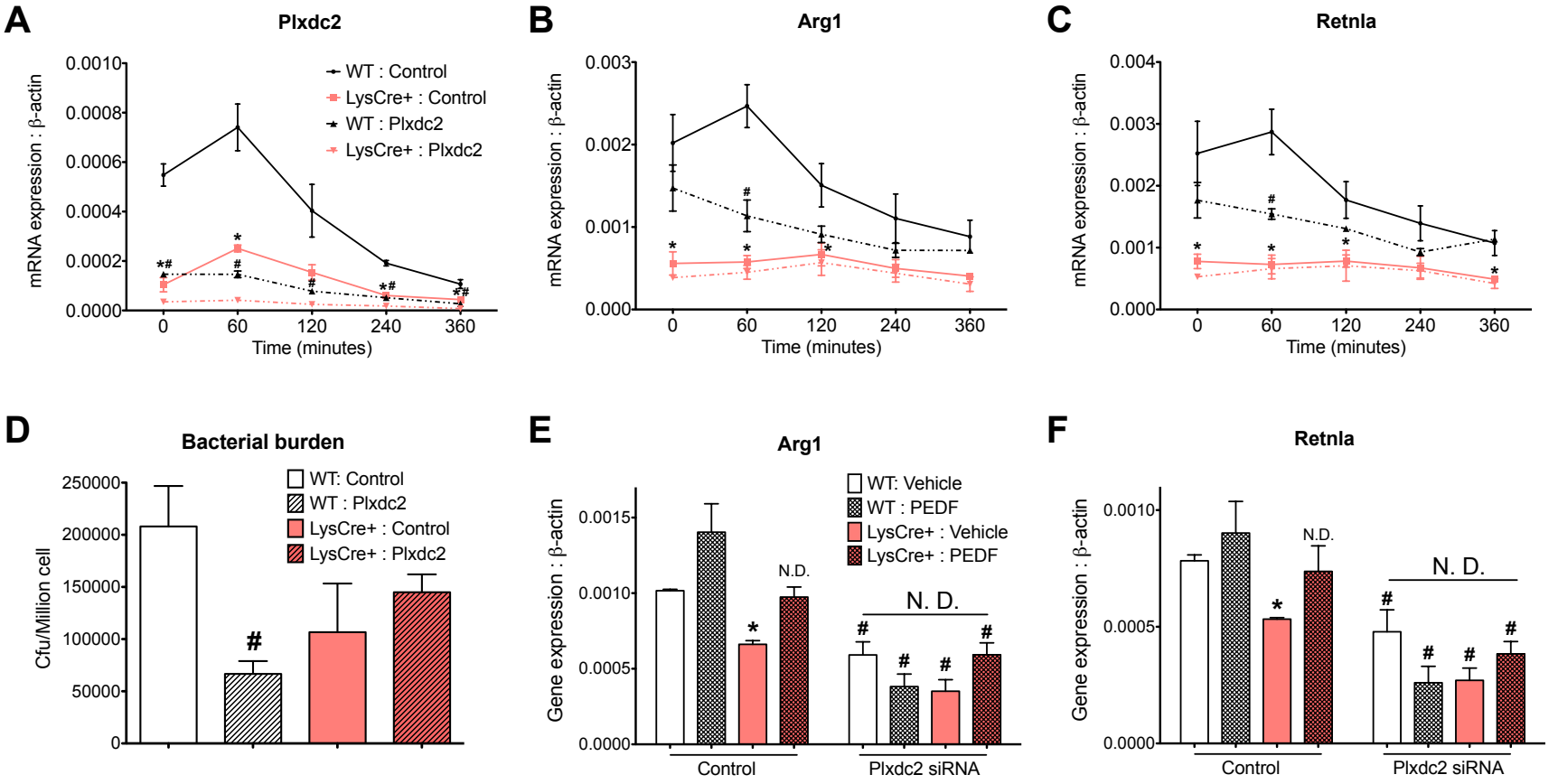
A
Plxdc2
mRNA expression : β-actin
0.0010
0.0008
0.0006
0.0004
0.0002
0.0000
WT : Control
LysCre+ : Control
WT : Plxdc2
LysCre+ : Plxdc2
0
60
120
240
360
Time (minutes)
B
Arg1
mRNA expression : β-actin
0.003
0.002
0.001
0.000
Time (minutes)
C
Retnla
mRNA expression : β-actin
0.004
0.003
0.002
0.001
0.000
Time (minutes)
D
Bacterial burden
Cfu/Million cell
250000
200000
150000
100000
50000
0
WT: Control
WT : Plxdc2
LysCre+ : Control
LysCre+ : Plxdc2
E
Arg1
Gene expression : β-actin
0.0015
0.0010
0.0005
0.0000
WT: Vehicle
WT : PEDF
LysCre+ : Vehicle
LysCre+ : PEDF
N.D.
N. D.
Control
Plxdc2 siRNA
F
Retnla
Gene expression : β-actin
0.0010
0.0005
0.0000
N.D.
N. D.
Control
Plxdc2 siRNA

Gene Symbol	Gene Full Name	Number of publications	Cellular Location	Function/Role	Ligands
Plxdc2	Plexin domain containing 2	3 (22)	Plasma membrane	PEDF receptor (IL-10 expression). Nervous system development	PEDF
Ppp1r3e	Protein phosphatase 1, regulatory (inhibitor) subunit 3E	1	Cytoplasm	Glycogen metabolism (increases glycogen synthesis).	None
Vsig8	V-set and immunoglobulin domain containing 8	2	Plasma membrane	Expressed in hair shaft, follicle, nail unit, and oral cavity. VISTA receptor (potential target for cancer or infectious disease)	VISTA (not commercialized)
Ankrd29	Ankyrin repeat domain 29	1	Nucleus	Niemann-Pick Type C diseases (lipid transport)	None
C1qtnf1	C1q and tumor necrosis factor related protein 1	24 (27)	Cytoplasm, nucleus	Adipokyne related to glucose metabolism. Link to Pparγ (increased expression with rosiglitazone treatment).	None